

# Predator-scale spatial analysis of intra-patch prey distribution reveals the energetic drivers of rorqual whale super-group formation

David E. Cade<sup>1,2</sup>  | S. Mduduzi Seakamela<sup>3</sup>  | Ken P. Findlay<sup>4,5</sup>  | Julie Fukunaga<sup>1</sup> | Shirel R. Kahane-Rapport<sup>1</sup>  | Joseph D. Warren<sup>6</sup>  | John Calambokidis<sup>7</sup> | James A. Fahlbusch<sup>1,7</sup>  | Ari S. Friedlaender<sup>2</sup>  | Elliott L. Hazen<sup>8</sup>  | Deon Kotze<sup>3</sup>  | Steven McCue<sup>3</sup>  | Michael Meyer<sup>3</sup>  | William K. Oestreich<sup>1</sup>  | Machiel G. Oudejans<sup>9</sup>  | Christopher Wilke<sup>10</sup> | Jeremy A. Goldbogen<sup>1</sup> 

<sup>1</sup>Hopkins Marine Station, Stanford University, Pacific Grove, CA, USA; <sup>2</sup>Institute of Marine Science, University of California, Santa Cruz, Santa Cruz, CA, USA; <sup>3</sup>Department of Environment, Forestry and Fisheries, Branch: Oceans and Coasts, Victoria & Alfred Waterfront, Cape Town, South Africa; <sup>4</sup>Oceans Economy, Cape Peninsula University of Technology, Cape Town, South Africa; <sup>5</sup>MRI Whale Unit, Department of Zoology and Entomology, University of Pretoria, Hatfield, South Africa; <sup>6</sup>School of Marine and Atmospheric Sciences, Stony Brook University, Southampton, NY, USA; <sup>7</sup>Cascadia Research Collective, Olympia, WA, USA; <sup>8</sup>Environmental Research Division/Southwest Fisheries Science Center/National Marine Fisheries Service/National Oceanic and Atmospheric Administration, Monterey, CA, USA; <sup>9</sup>Kelp Marine Research, Hoorn, The Netherlands and <sup>10</sup>Department of Environment, Forestry and Fisheries, Branch: Fisheries Management, Cape Town, South Africa

## Correspondence

David E. Cade

## Funding information

Office of Naval Research, Grant/Award Number: N000141612477; Stanford University; South African Department of the Environment, Forestry and Fisheries; National Science Foundation, Grant/Award Number: 1656691

**Handling Editor:** Daniel Crocker

## Abstract

1. Animals are distributed relative to the resources they rely upon, often scaling in abundance relative to available resources. Yet, in heterogeneously distributed environments, describing resource availability at relevant spatial scales remains a challenge in ecology, inhibiting understanding of predator distribution and foraging decisions.
2. We investigated the foraging behaviour of two species of rorqual whales within spatially limited and numerically extraordinary super-aggregations in two oceans. We additionally described the lognormal distribution of prey data at species-specific spatial scales that matched the predator's unique lunge-feeding strategy.
3. Here we show that both humpback whales off South Africa's west coast and blue whales off the US west coast perform more lunges per unit time within these aggregations than when foraging individually, and that the biomass within gulp-sized parcels was on average higher and more tightly distributed within super-group-associated prey patches, facilitating greater energy intake per feeding event as well as increased feeding rates.
4. Prey analysis at predator-specific spatial scales revealed a stronger association of super-groups with patches containing relatively high geometric mean biomass and low geometric standard deviations than with arithmetic mean biomass, suggesting that the foraging decisions of rorqual whales may be more influenced by the distribution of high-biomass portions of a patch than total biomass. The hierarchical distribution of prey in spatially restricted, temporally transient, super-group-associated

[Correction note added on 25-February 2021, after first online publication: The second author in the How to cite this article box has been amended.]

patches demonstrated high biomass and less variable distributions that facilitated what are likely near-minimum intervals between feeding events.

- Combining increased biomass with increased foraging rates implied that overall intake rates of whales foraging within super-groups were approximately double those of whales foraging in other environments. Locating large, high-quality prey patches via the detection of aggregation hotspots may be an important aspect of rorqual whale foraging, one that may have been suppressed when population sizes were anthropogenically reduced in the 20th century to critical lows.

#### KEYWORDS

blue whales and humpback whales, fisheries acoustics, foraging ecology, gulp-sized cell, lognormal prey distribution, patchiness, raptorial filter-feeding, whale scale

## 1 | INTRODUCTION

Both the density of foraging predators and the types of collective behaviours displayed by groups are strongly driven across taxa by the heterogeneity, or patchiness, of resources in the environment (Gordon, 2014; Piatt & Methven, 1992), but effectively describing the availability of patchy resources to foragers is a fundamental challenge in ecology (Benoit-Bird et al., 2013; Chave, 2013; Levin, 1992). Baleen whale (parvorder: Mysticeti) predator/prey systems are ideal for investigating the physiological drivers and ecological limits related to patchiness because, as capital-breeding bulk filter-feeders, baleen whales require dense concentrations of seasonally available prey; essentially, their life history is driven by both spatial (Hazen et al., 2009, 2015; van der Hoop et al., 2019; Piatt & Methven, 1992) and temporal patchiness (Abrahms et al., 2019; Fossette et al., 2017). Additionally, unusually in pelagic systems it is possible to study both the behaviour of baleen whales and the distribution of their euphausiid (krill) prey quantitatively and simultaneously *in situ* via the use of bio-logging tags and hydroacoustic echosounders (e.g. Baumgartner & Mate, 2003; Goldbogen et al., 2019; Guilpin et al., 2019; Owen et al., 2017).

Baleen whales are the largest predators of all time, and rorqual whales (in the clade Balaenopteroidea) including blue whales *Balaenoptera musculus* and humpback whales *Megaptera novaeangliae* can engulf volumes of water (means ~130 and 15 m<sup>3</sup> respectively) that approach or exceed their own body masses (Goldbogen et al., 2012; Kahane-Rappaport & Goldbogen, 2018). Most typically, lunge-filter-feeding whales forage singly or in small groups ( $\leq 3$  animals), and large groups of up to 10–20 animals, often fish-feeding humpback whales, have also been reported in some ecosystems (Jurasz & Jurasz, 1979; Kirchner et al., 2018; Whitehead, 1983). Group membership can be defined spatially or behaviourally according to the process under study (Mann, 2000); here we refer to groups as spatially cohesive aggregations, regardless of social, temporal or behavioural affiliations, such that individuals must interact with each other (constructively or destructively) when accessing prey. Topographical or transient oceanographic features (i.e. bays, fronts and upwelling regions) are sometimes associated with very large numbers (200+) of animals distributed over large (10–70 km) spatial extents that can generally be considered to

be foraging independently of each other (e.g. Jaquet, 1996; Nowacek et al., 2011). In contrast, our study involves dense aggregations such that individuals could be in direct conflict for the same resource.

The formation of spatially constricted, large aggregations of humpback whales in close proximity (numbering upwards of 100 whales within five body lengths) have been observed since 2011 in the Benguela Current upwelling region off the west coast of South Africa in a region where previous studies reported only loose aggregations up to 20 animals (Findlay et al., 2017). Known as super-groups, similarly large aggregations have been reported historically (e.g. Bruce, 1915), and the contemporary re-emergence of this behaviour may be related to the recovery of regional large whale populations above critical thresholds. Findlay et al. (2017) relate that animals in these super-groups are likely foraging; however, group behaviour does not necessarily imply optimal behaviour (Przybylski et al., 2013), and the proximate causes that inspire such large aggregations have not before been explained.

In this study, we examined the prey conditions near, and the foraging behaviour of, large aggregations of rorqual whales in two environments: humpback whales in South Africa and blue whales in Monterey Bay off the US west coast (Figure 1). We hypothesized that the whales observed in super-groups were foraging throughout the environment in which they were observed, but that foraging conditions were of higher quality proximal to super-group observations, suggesting that prey availability is an underlying driver of super-group aggregation. To test this hypothesis, we characterized the prey fields in both environments proximal to foraging whales that were both loosely and densely aggregated by analysing fisheries acoustics data at spatial scales that match the foraging style of the predators. We show how this method can be used to reveal differences between heavily foraged patches proximal to large predator aggregations and other patches in the environment that also appear to contain abundant biomass. We additionally used bio-logging tags in both environments to test whether whales in super-groups demonstrated higher feeding rates than whales not aggregated in super-groups. Illuminating the differences in prey conditions between aggregated and non-aggregated whales may not only explain why super-groups form,

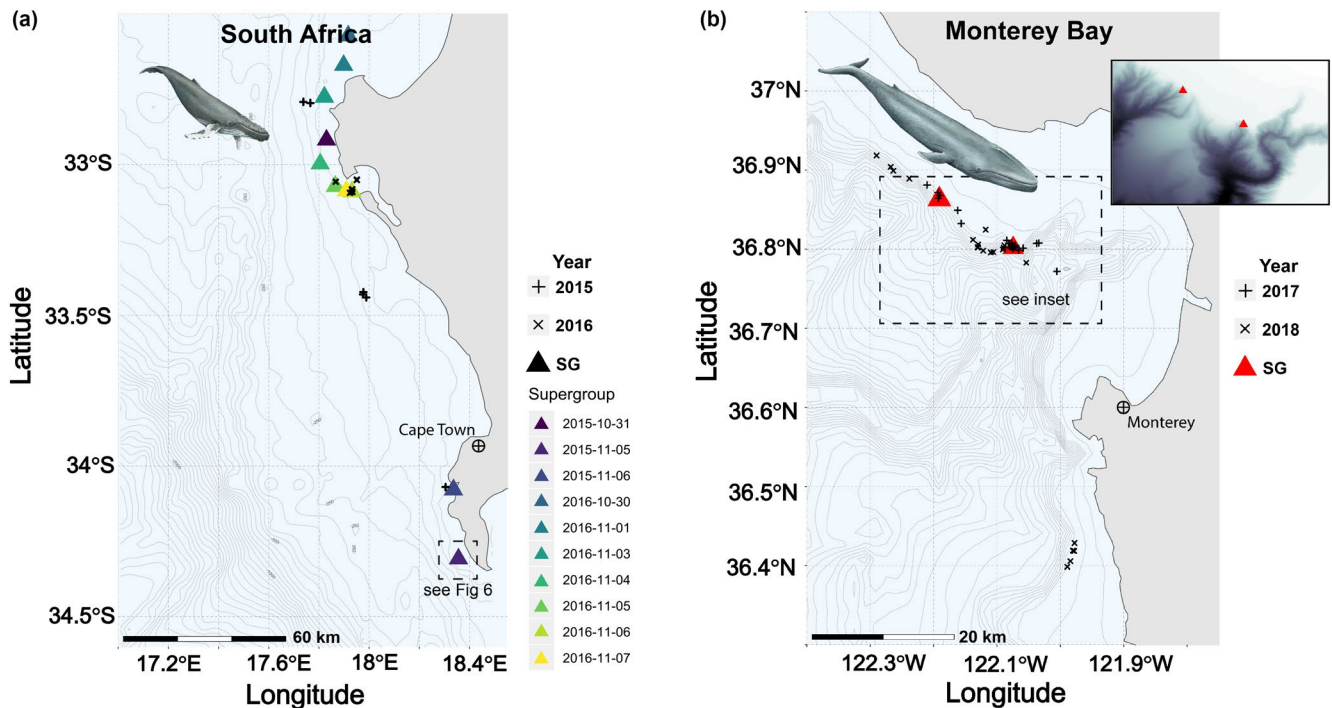


**FIGURE 1** Field locations in South Africa (a) and Monterey Bay (b). Depth contour lines are separated by 50 m until the 500-m isobath and then 100 m thereafter. Triangles show observed super-group (SG) locations, and + and × mark the deployment locations of suction-attached bio-loggers on humpback (a) and blue whales (b). Data collected near each super-group are collated in Table S1

but may aid understanding about how predators foraging in a patchy environment make decisions about where and when to expend foraging effort.

## 2 | MATERIALS AND METHODS

We investigated aggregations of rorqual whales in two eastern boundary current upwelling ecosystems: humpback whales in the Benguela Current off South Africa's west coast in 2015 and 2016, and blue whales in Monterey Bay off the US west coast in 2017 and 2018 (Figure 1). These aggregations are distinct from other contemporary descriptions of large baleen whale groups in the extraordinary density of animals within a small region of open ocean—in the case of humpback whales including up to 200 individuals within regions as small as 200 m on a side (Findlay et al., 2017)—such that animals must interact with each other as they are foraging (Figure 2, Video S1). While humpback whale super-groups were the specific focus of research efforts in South Africa, large aggregations of blue whales were encountered only twice opportunistically during Monterey Bay field efforts. For detailed field methods, see Appendix S1.

### 2.1 | Foraging behaviour

In both locations, to examine foraging behaviour within and outside of super-groups, we attached integrated 3D accelerometer

and video tags to whales for time periods of ~2–20 hr. Individual feeding events that involve engulfing a mass of water and krill that can exceed the size of the whale (hereafter, 'lunges' or 'gulps', see Goldbogen et al., 2017) were identified via their kinematic signatures (as in Cade et al., 2016). Foraging behaviours including feeding rate (lunges/hr), inter-lunge interval, foraging bout length and foraging depth were compared within species between super-group and non-super-group times (details in Appendix S1), as well as between the two study ecosystems and among other ecosystems with krill-feeding whales of the same species (total of 112 blue whales and 45 humpback whales, Table 1).

To determine the significance of comparisons between super-group and non-super-group foraging of tagged animals, both *t*-tests and generalized linear mixed effects (GLME) models were used. Foraging of tagged whales when they were and were not in super-groups was compared, and super-group foraging was additionally compared to other whales in the same environment but not in super-groups. Finally, super-group foraging was compared to a larger population of whales outside the specific tagging period. For humpback whales, this was all krill-feeding whales from California, the Antarctic and South Africa. For blue whales, this was a comparison with blue whales in the same region as the super-group (Monterey Bay) but a year later. *T*-tests were used to test for significant differences between mean feeding rates (lunges/hr during foraging bouts) of super-group whales and mean feeding rates of whales foraging when not aggregated in super-groups (Table 2; Table S2). For both species, foraging bouts were defined as the time period that included all foraging dives with <5.5 min (see Appendix S1 and

**FIGURE 2** Investigating super aggregations of predators and prey. (a) UAV image of at least 60 humpback whales off South Africa's west coast, scale is estimated from mean humpback whale length (image© Jean Tresfon). (b) UAV image of four blue whales in an aggregation of ~15 whales in Monterey Bay, CA (image© Duke Marine Robotics and Remote Sensing). Inset: map of super-group region with tracks of tagged whales; the green track represents the topmost whale in the image. (c, d) Underwater views of multiple humpback and blue whales, respectively, feeding simultaneously. (e, f) Acoustic backscatter near super-group in South Africa and Monterey Bay, respectively, overlaid with the time-synched depth profiles and lunges (green circles) of whales tagged nearby. Grid lines are sized to match the dive-scale unit of analysis for each species

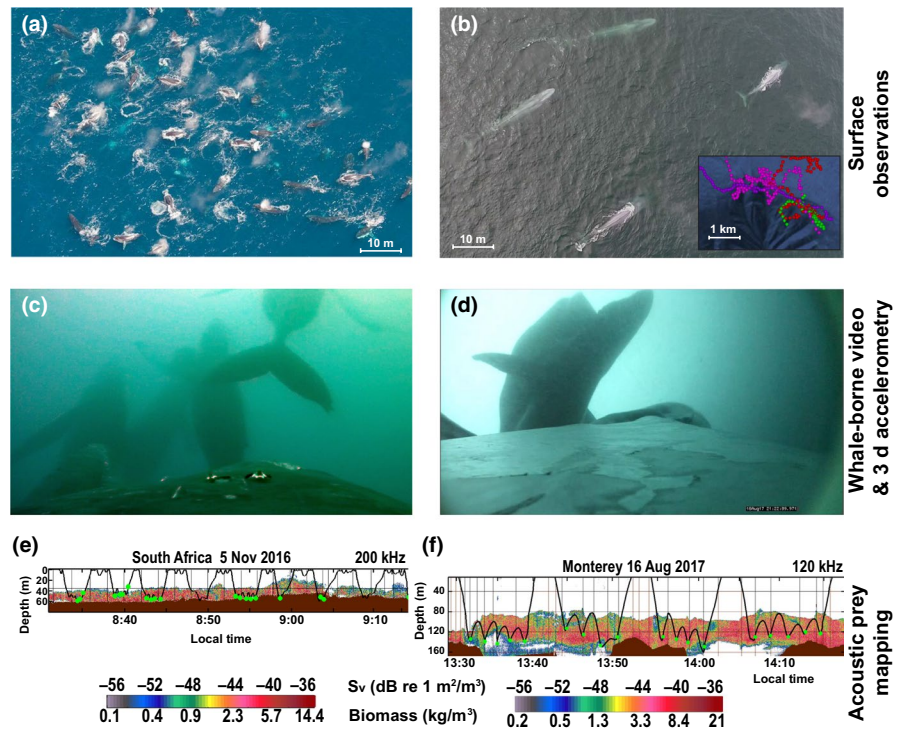


**TABLE 1** Morphometric and feeding parameters that informed analysis, using all krill-feeding whales from (Goldbogen et al., 2019). Body lengths are representative of whales in the region. Ventral Groove Blubber length ( $VGB_L$ ) and jaw length ( $Jaw_L$ ) were allometrically determined (Kahane-Rapport & Goldbogen, 2018) and used to create the gulp-size cell (Figures 3 and 4). Search areas were used to calculate the size of the dive-sized cells

Species	Length	$VGB_L$	$Jaw_L$	Vertical search area	Horizontal search area	Inter-lunge interval	Lunges per dive	Deployments
<i>Balaenoptera musculus</i>	22.5 m	12.8 m	4.25 m	$44 \pm 16 \text{ m}^3$	$240 \pm 119 \text{ m}^3$	$108 \pm 254 \text{ s}$	$3.3 \pm 2.0$	112
<i>Megaptera novaeangliae</i>	10.5 m	6.0 m	2.25 m	$35 \pm 20 \text{ m}^3$	$125 \pm 99 \text{ m}^3$	$43 \pm 12 \text{ s}$	$3.2 \pm 1.1$	45

<sup>a</sup>Search areas for *B. m.* were limited to deployments with georeferenced pseudotracks ( $n = 51$ ).

Figure S4) from the return to the surface of one foraging dive to the start of the next foraging dive. GLME models were constructed in Matlab 2019a for inter-lunge interval (ILI), lunges per dive, dive duration and search area from all data using super-group status as a fixed effect and individual whale as a random effect. For dive duration and lunges per dive, factors known to be influenced by dive depth, mean lunge depth for each dive was binned into 50-m depth bins and used as an additional random effect.

**2.2 | Prey data collection and initial processing**

Prey data were collected using multi-frequency (38 and either 120 or 200 kHz), split-beam fisheries acoustic systems (Simrad EK60s or EK80s) ensonifying the water column below a vessel within an estimated 500 m of foraging whales in both ecosystems, a distance we considered proximal given the size of observed patches. Data collected near super-groups were compared to data collected near feeding whales not aggregated into super-groups on each observation day and in aggregate as described below. Krill biomass at each

analysed spatial scale was estimated from the mean volume back-scattering strength ( $S_v$  in  $\text{dB re } 1 \text{ m}^2/\text{m}^3$ , Table 3) of pings aggregated into cells in Echoview v9 with heights and lengths as detailed below. The acoustic set-up, the calculation of target strength for small krill and the conversion of acoustic units to biomass units are all detailed in Appendix S1. Aggregations of krill, dominated by large swarms >10 m thick and 1 km across, were identified in acoustic echograms using the SHAPES school detection algorithm (Barange, 1994; Coetzee, 2000) and dB differencing techniques (Jarvis et al., 2010, additional details in Appendix S1).

**2.3 | Predator-scale prey analysis**

Rorqual whales utilize a unique foraging style, lunge-filter-feeding, characterized by raptorial targeting of discrete parcels of water followed by filtration through baleen plates and retention of prey (Goldbogen et al., 2017; Pivorunas, 1979). Typically this behaviour consists of diving to depths ranging from the surface to >300 m, performing one to ten lunges, and then returning to the surface to

**TABLE 2** Mean feeding parameters derived from tag data for whales foraging in super groups (SG) and not in super groups (NSG). Feeding bout definition described in Figure S4. Data for individual whales foraging in super-groups ( $n = 6$  in both ecosystems) in Table S2. *M. n.* = *M. novaeangliae* (humpback whales), *B. m.* = *B. musculus* (blue whales)

	Feeding rate (lunges per hr within a foraging bout)		Inter lunge interval (ILI, s)		Inter lunge search area ( $10^2 \text{ m}^2$ )		Lunges per dive	
	SG	NSG	SG	NSG	SG	NSG	SG	NSG
<b><i>Megaptera novaeangliae</i> (South Africa)</b>								
SG animals	55 ± 15	37 ± 18	32 ± 10	40 ± 18	3.4 ± 2.5	8.1 ± 11	4.5 ± 1.5	3.6 ± 2.2
( <i>p</i> -value)	(0.078)		***(0.000)		***(0.000)		(0.516)	
Number of animals	6	5	6	5	6	3	6	5
All SA <i>M. n.</i>	55 ± 15	39 ± 15	32 ± 10	36 ± 16	3.4 ± 2.5	6.6 ± 10	4.5 ± 1.5	4.1 ± 2.5
( <i>p</i> -value)	(0.086)		***(0.000)		***(0.000)		(0.492)	
Number of animals	6	7	6	7	6	5	6	7
All <i>M. n.</i>	55 ± 15	38 ± 16	32 ± 10	44 ± 18	3.4 ± 2.5	11 ± 26	4.5 ± 1.5	4.4 ± 2.1
( <i>p</i> -value)	*(0.028)		***(0.000)		** (0.006)		(0.913)	
Number of animals	6	17	6	33	6	30	6	33
<b><i>Balaenoptera musculus</i> (Monterey Bay)</b>								
SG animals	24 ± 2.9	21 ± 5.1	95 ± 17	102 ± 19	36 ± 34	42 ± 40	4.0 ± 0.9	3.3 ± 1.3
( <i>p</i> -value)	(0.214)		(0.187)		(0.083)		(0.387)	
Number of animals	6	5	6	5	6	5	6	5
All MRY 2017 <i>B. m.</i>	24 ± 2.9	22 ± 3.9	95 ± 17	101 ± 16	36 ± 34	42 ± 32	4.0 ± 0.9	3.3 ± 1.3
( <i>p</i> -value)	(0.200)		(0.126)		*(0.028)		*(0.038)	
Number of animals	6	17	6	17	6	17	6	17
SG <i>B. m.</i> versus 2018 <i>B. m.</i>	24 ± 2.9	18 ± 3.1	95 ± 17	108 ± 22	36 ± 34	57 ± 85	4.0 ± 0.9	4.8 ± 1.4
( <i>p</i> -value)	***(0.000)		*(0.014)		(0.124)		(0.886)	
Number of animals	6	22	6	22	6	22	6	22

\* $p < 0.05$ , \*\* $p < 0.01$ , \*\*\* $p < 0.001$ .

breathe before diving again. To match the spatial scale of prey analysis to the spatial scale utilized by diving whales, we first used tag data to identify the mean horizontal and vertical distances travelled by foraging whales of both study species from 10 s before the first lunge in a dive to 10 s after the last lunge in a dive (distances in Table 1, details in Appendix S1). We then divided the acoustically identified prey patches (Figures 3a and 4c–d) into these dive-sized cells (Figures 3b and 4e–f).

To examine the distribution of krill within dive-sized cells (Figure 3c and 4h), we used Echoview to calculate  $S_v$  within analytical cells the size of an average whale engulfment volume ( $S_{v\_gulp}$ , symbol definitions in Table 3) as calculated from the morphology of an intermediately sized representative of each species of interest (blue whale total length = 22.5 m, humpback whale = 10.5 m). Jaw length was used for the vertical size of the cell (blue whale = 4.3 m, humpback whale = 2.3 m), and the ventral groove blubber length (blue whale = 12.8 m, humpback whale = 6.0 m) was used for the horizontal cell size (lengths calculated from ordinary least squares regression relationships in Kahane-Rapport & Goldbogen, 2018). At the observed prey patch depths, all return echoes had y-axis values larger than the head width, so the extracted cells represented a 2D projection of the gulp size. The engulfed water volume of

rorqual whales is a good spatial match for the analysis of acoustic data since the large size of engulfed water parcels allows multiple acoustic returns to be processed even at our smallest desired spatial scale. Gulp-sized cells contained a minimum of two pings, and in Monterey, blue whale gulp-sized cells averaged  $9.4 \pm 12.5$  pings (mean  $\pm$  SD), while in South Africa humpback whale gulp-sized cells averaged  $8.4 \pm 6.8$  pings (details in Appendix S1). The variation in the number of pings per gulp is a product of variable speeds by the survey vessel and variable ping rates set to maximize the number of samples without introducing acoustic artefacts like false bottoms. When such variation is present in a survey, data that are averaged into patches without first accounting for survey distance can potentially be biased. We report whole patch  $S_v$  (e.g. Figure 4c,d; Table S3) for comparison to the spatially averaged approach described above.

## 2.4 | Characterizing patchy prey

In both marine (Bennett & Denman, 1985; Campbell, 1995) and terrestrial (White, 1978) environments, both inter- (Magurran & Henderson, 2003; Pagel et al., 1991; Preston, 1948, 1962) and intra- (Anand & Li, 2001; Barnes, 1952) species abundances tend to be

**TABLE 3** Definitions of symbols and abbreviations. See Figure 3 for schematic representation of hierarchical prey distribution calculations. Subscripts LN or N before the variable denote lognormal or normal distributions respectively. See MacLennan et al. (2002) for further descriptions of  $S_v$  and TS. For further discussion of the calculation of  $\hat{B}$  or  $\hat{S}_v$ , see Appendix S1 section 'Estimating overall intake'. See equation 1 in Appendix S1 for information on calculating  $B$  from  $S_v$

Symbol	Definition	Units	Scale
$\cdot$ , $:$	Multiply or divide (the multiplicative correlate to $\pm$ )	–	–
$B_{\text{gulp}}$	Biomass density within a gulp-sized cell	kg/m <sup>3</sup>	Gulp
$B_{\text{patch}}$	Arithmetic mean biomass density within a patch (estimated from $S_{v_{\text{patch}}}$ )	kg/m <sup>3</sup>	Patch
${}^{\text{LN}}B_{\text{ws}}$	Whale scale biomass: the distribution of $B_{\text{gulp}}$ within a dive-sized cell, estimated from ${}^{\text{N}}S_{v_{\text{ws}}}$ and equivalent to $\text{geomean}(B_{\text{gulp}}) \cdot \text{GSD}(B_{\text{gulp}})$	kg/m <sup>3</sup>	Dive
$\overline{{}^{\text{LN}}B_{\text{ws}}}$	Distribution of ${}^{\text{LN}}B_{\text{ws}}$ within a patch or region, estimated from $\overline{{}^{\text{N}}S_{v_{\text{ws}}}}$ and equivalent to $\text{geomean}({}^{\text{LN}}B_{\text{ws}}) \cdot \text{GSD}({}^{\text{LN}}B_{\text{ws}})$	kg/m <sup>3</sup>	Patch or region
$\hat{B}$	Estimated arithmetic mean biomass (mean biomass consumed over time) calculated the summary variables $\text{geomean}(B_{\text{ws}})$ and $\text{GSD}(B_{\text{ws}})$	kg/m <sup>3</sup>	Dive, patch or region
geomean	Geometric mean	–	–
GSD	Geometric standard deviation	–	–
SD	Standard deviation	–	–
$S_v$	Mean volume back scatter strength (MVBS)	dB re 1 m <sup>2</sup> /m <sup>3</sup>	–
$S_{v_{\text{gulp}}}$ or $S_{v_{\text{gulp}}}$	MVBS within a gulp-sized cell	dB re 1 m <sup>2</sup> /m <sup>3</sup>	Gulp
$S_{v_{\text{patch}}}$ or $S_{v_{\text{patch}}}$	MVBS within a patch	dB re 1 m <sup>2</sup> /m <sup>3</sup>	Patch
$S_{v_{\text{dive}}}$ or $S_{v_{\text{dive}}}$	MVBS within a dive-sized cell	dB re 1 m <sup>2</sup> /m <sup>3</sup>	Dive
${}^{\text{N}}S_{v_{\text{ws}}}$ or ${}^{\text{N}}S_{v_{\text{ws}}}$	Whale scale $S_v$ : the distribution of $S_{v_{\text{gulp}}}$ within a dive-sized cell, presented as $\text{mean}(S_{v_{\text{gulp}}}) \pm \text{SD}(S_{v_{\text{gulp}}})$	dB re 1 m <sup>2</sup> /m <sup>3</sup>	Dive
$\overline{{}^{\text{N}}S_{v_{\text{ws}}}}$ or $\overline{{}^{\text{N}}S_{v_{\text{ws}}}}$	Distribution of $\text{mean}({}^{\text{N}}S_{v_{\text{ws}}})$ of all dive-sized cells within a patch or region, presented as $\text{mean}({}^{\text{N}}S_{v_{\text{ws}}}) \pm \text{SD}({}^{\text{N}}S_{v_{\text{ws}}})$	dB re 1 m <sup>2</sup> /m <sup>3</sup>	Patch or region
$\hat{S}_v$	Estimated MVBS from a dive, patch or region, calculated from the summary variables $\text{mean}(S_v)$ and $\text{SD}(S_v)$	dB re 1 m <sup>2</sup> /m <sup>3</sup>	Dive, patch or region
TS	Target strength (see equation 1 in Appendix S1)	dB re 1 m <sup>2</sup>	–

distributed heterogeneously and can often be characterized by log-normal distributions (Dennis & Patil, 1987). That is, the log of abundance data is typically normally distributed and can be characterized by the mean and standard deviation of logged data, or, equivalently, the geometric mean and geometric standard deviation of the unlogged data. Fisheries acoustics data, however, are typically reported as overall mean abundance integrated over broad areas (e.g. Benson et al., 2002; Cox et al., 2009; Croll et al., 1998; Nickels et al., 2019) or mean volumetric density within patches (e.g. Hazen et al., 2015; Nowacek et al., 2011; Owen et al., 2017). Prey patches can be heterogeneously distributed in space (Benoit-Bird et al., 2019; Kaartvedt et al., 2005; Watkins & Murray, 1998), however, and aggregations themselves can have variable structure (Benoit-Bird et al., 2017), implying that using a single number to characterize the biomass density of a large patch may not represent what a foraging animal encounters

(Stephens & Krebs, 1986). Additionally, averaging the biomass densities among patches with variable sizes may misrepresent mean availability if biomass is not weighted by patch size, or if acoustic surveys with variable ping rates or vessel speeds are not first averaged into spatially consistent regions.

When prey patches are small such that a lunge-feeding whale feeds on it only once, describing patch density with a single number for each krill patch would be an appropriate strategy. However, the krill swarms we observed in this study were several kilometres across (Figure 2) such that predators could be considered to be foraging within a patch rather than among patches. Consequently, to better represent the prey biomass available to foraging rorqual whales, we characterized the prey fields proximal to feeding whales at predator-specific spatial scales, dividing large patches into analytical cells the size of an individual whale's gulp and then examining how those gulp-sized cells are

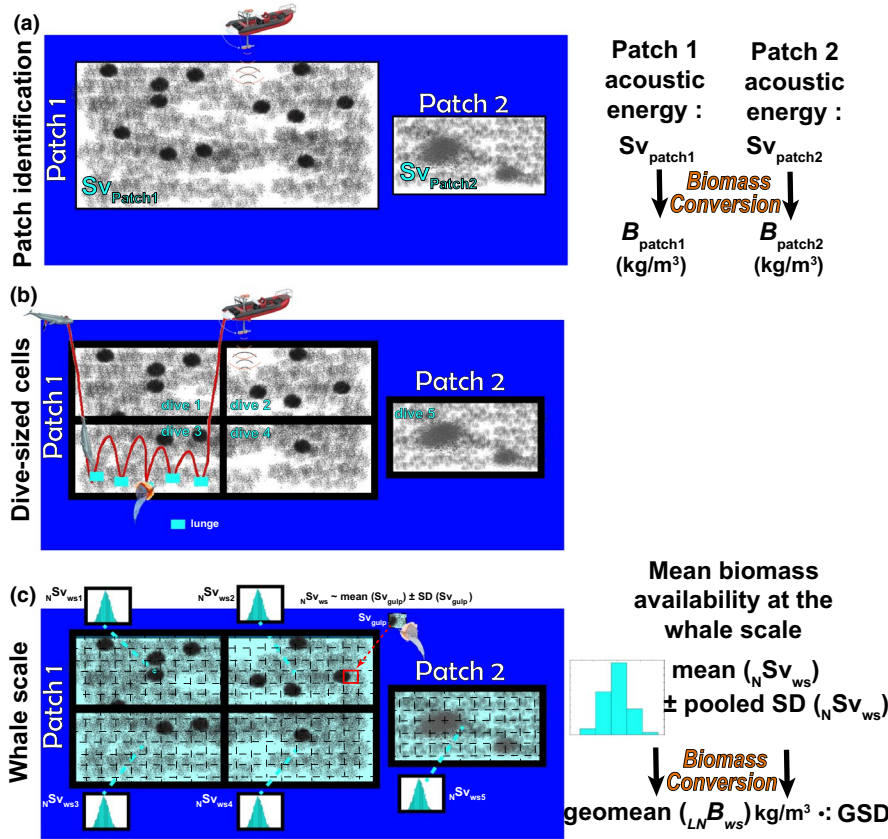


**FIGURE 3** Schematic illustrating the analytical technique for two acoustically detected prey patches. (a) The patch scale is commonly reported in acoustics literature, looking at the linearly averaged mean biomass within each patch. (b) In the whale-scale approach, patches are first divided into cells the size of an average whale foraging dive (Table 1). (c) The whale scale looks at the distribution of the biomass of gulp-sized cells within dives and then pools results for a representation of the mean availability of biomass at the scale experienced by the predator. Biomass conversion equation in Appendix S1, equation 1. *SD* = standard deviation, *geomean* = geometric mean =  $\text{antilog}(\text{mean}(\log(\text{biomass})))$ , *GSD* = geometric standard deviation =  $\text{antilog}(SD(\log(\text{biomass})))$ . Other symbols defined in Table 3

distributed within cells of a size likely experienced by whales on a foraging dive (Figures 3 and 4). These gulp-sized cells are distributed, as in patchy prey in other aquatic and terrestrial systems, lognormally (more details in Appendix S1, Figure S1). Details for estimating mean intake from lognormal distributions are also reported in the Appendix S1 section ‘Estimating overall intake’.

### 2.5 | The whale scale

For each dive-sized cell in a region of interest (e.g. all dive-sized cells proximal to a super-group on a specific day), we first summarized the distribution of biomasses likely to be experienced by a foraging whale on a dive by calculating the mean and standard deviation (*SD*) of  $S_{v\_gulp}$  within each dive-sized cell. To ensure sufficient statistical power, only cells that had at least 30 gulp-sized cells were included in analysis. We then summarized the overall distribution in super-group-associated patches and patches not associated with super-groups by averaging all dive summary values ( ${}_N S_{v_{ws}}$ ) in a region and calculating the pooled *SD* of all dives within the region of interest (Figure 3c). We refer to this summarized analysis of prey as the mean ‘whale scale’ ( $\overline{{}_N S_{v_{ws}}}$  in acoustic units,  $\overline{{}_{LN} B_{ws}}$  in estimated biomass units, Table 3).

All statistical comparisons were done on the acoustic units which have approximately normal distributions, and then  $S_v$  was converted to estimated biomass (generally following Jarvis et al., 2010, with study-system-specific calculation details in Appendix S1). Because biomass estimation is subject to model enhancements over time, we report  $S_v$

(as  $\text{mean} \pm \text{pooled } SD$ ) throughout the text in addition to biomass ( $B$ , Table 3). Biomass of gulp-sized cells ( $B_{gulp}$ ) was lognormally distributed at larger scales (Figure S1), so for whale-scale summary values we present the geometric mean (*geomean*) and the geometric standard deviation (*GSD*) of gulp-sized cells ( $B_{gulp}$ ). The *geo*

mean and *GSD* are equivalent to the antilog of the mean and *SD* of  $\log(\text{biomass})$ . There are several advantages to summarizing data using lognormal distributions instead of reporting mean biomass including less sensitivity to outliers and a better ability to characterize the spread of data. We report lognormal summary statistics as ‘biomass in  $kg/m^3 \cdot$  a multiplicative scalar’, where  $\cdot$  is read ‘multiplied or divided by’ and is a combination of the multiplication ( $\cdot$ ) and division ( $\div$ ) symbols introduced by Leibniz (1684).  $\cdot$  can be interpreted as the multiplicative complement to the commonly used  $\pm$ .

The whale scale analytical scale—the distribution of gulp-sized cells within their containing dive-sized cell (Figures 3c and 4e,f)—can be thought of as the spread of biomass around a dive’s median biomass. We developed this scale because of its link to the spatial scale of prey experienced by foraging rorqual whales on any given foraging dive. This analytical technique gives a representation of what a foraging rorqual could encounter on a dive and would represent what it is likely to forage on if it forages indiscriminately during its dive. However, to account for the likelihood that rorquals employ an active selection strategy to maximize their prey intake, we additionally analysed the distribution of only the top 50% of gulp-sized cells within dive-sized cells. The choice of 50% as a threshold was selected as a compromise between indiscriminate feeding centred

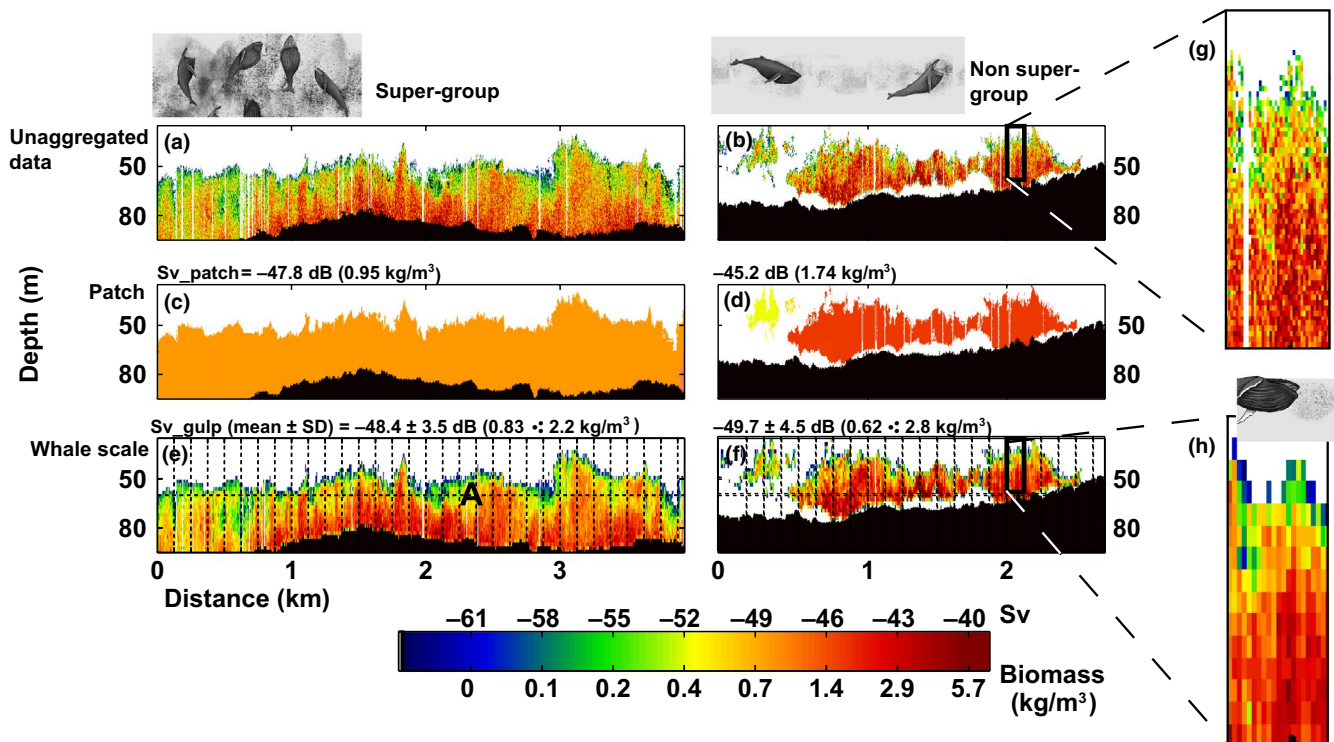


**FIGURE 4** Matching the spatial scale of rorqual whale feeding with acoustic analysis can illuminate differences between patches that appear to be of similar quality. (a, b) Hydroacoustic data from super-group and non-super-group regions on 5 November 2015, averaged into 1 m × 1 m cells (for display purposes along a consistently sized x-axis). (c, d) The mean density of each identified krill swarm as exported from Echoview. The large non-super-group krill swarm in d had nearly double the krill density overall than the swarm in c proximate to a super-group, suggesting that the mean density of krill swarms may not be an appropriate metric to describe prey availability here since at this scale the super-group patch would appear to be lower quality. (e, f) The whale scale: the patch is divided into cells the average size of a (2D) humpback whale foraging dive (125 m × 35 m) and then further divided into gulp-sized cells. The geometric mean of the gulp-sized cells within dive-sized cells is higher in the super-group proximal patch. (g) Acoustic data in a dive-sized cell at fine resolution. (h) Acoustic data in a dive-sized cell averaged into gulp-sized cells, demonstrating how at this resolution the distribution of krill within the patch is preserved

around a patch's median and precise selection of gulps with maximum density given how much is unknown about the behavioural patch selection algorithm employed by rorqual whales. We refer to this technique as the 'informed whale-scale' analysis and it can be thought of as the distribution of biomass around the 75th percentile of biomass in a dive-sized cell.

### 3 | RESULTS

Humpback whale super-groups off South Africa's west coast are described in detail in Findlay et al. (2017) and consist of 20–200 whales surfacing haphazardly in an area as restricted as 200 m on a side (Figure 2a; Video S1). Super-groups were observed on 10 of 20 ship days in 2015–2016 (Figure 1). The duration of super-group cohesiveness is unknown as none were observed from formation to dispersal, but all were observed for at least 1 hr and in all five instances where group dispersion was observed, emigration was sequential. Unlike in other environments where humpback whales have been observed coordinating their fish-feeding behaviour (Jurasz & Jurasz, 1979; Mastick, 2016; Wiley et al., 2011), underwater video evidence suggests that lunge feeding within these krill patches is uncoordinated

(e.g. Video S1). Two blue whale super-groups were encountered in 4 field days in 2017 in Monterey Bay, California, USA and consisted of an estimated 15–40 whales surfacing within sight of an observer at sea level (~1 km range); no super-groups were encountered in 9 field days in 2018. Blue whales generally forage in singles or in pairs and the super-groups we observed consisted of many singles and pairs feeding in the same area in an apparently uncoordinated fashion. Due to the similarities in behaviour and the much larger sizes of blue whales (blue whales are ~2× the length, 4× the mass and have 8× the engulfment capacity of humpback whales, Kahane-Rapport & Goldbogen, 2018), we propose that the observed group sizes are comparable despite their differences in individual predator abundances. The blue whale super-group encountered on August 14 (25–40 whales estimated) was encountered at 08:30 and had begun to decrease in density at ~11:15. On August 16, the group (15–20 whales estimated) was encountered at 13:30 and our vessels left the area at 14:20.

#### 3.1 | Foraging behaviour

All whales fed continuously (accounting for surface recovery and transit time) while in super-groups. Humpback whales fed at a mean

depth of  $43 \pm 13$  m while blue whales fed at  $109 \pm 30$  m (e.g. Figure 2). In both cases, whales in super-groups had similar lunges per dive as non-super-group whales (Table 2), but the smaller ILI and area traversed between lunges for whales in super-groups compared to non-super-groups (Table 2) led to shorter dive durations (model estimates accounting for foraging depth differences, blue whale 95% confidence interval (CI): 197 to 391 s shorter, humpback whale 95% CI: 60 to 112 s shorter). These factors combined to influence the overall feeding rate, as measured in lunges/hr during feeding bouts, which were 49 and 14% higher, respectively, in humpback whale and blue whale super-groups versus feeding rates when these same whales were not feeding in super-groups, and were 45 and 34% higher, respectively, when super-group whales were compared to krill-feeding whales more generally (Table 2). The increased feeding rates in super-groups suggested that we would find that prey near super-groups were distributed in such a way as to facilitate decreased search times.

### 3.2 | Prey analysis

Analysis of prey abundance and distribution revealed high-quality foraging conditions in both super-group and non-super-group behaviour states in each ecosystem. Identified prey patches near foraging whales were typically tens of metres thick and hundreds of metres wide, regardless of group size, such that whales could be described as foraging within a patch rather than among patches (Figure 2; Video S1). Examination of the distribution of the biomass of gulp-sized cells from all identified patches on each survey day revealed that the biomass density was distributed lognormally (Figure S1,

Appendix S1), suggesting the appropriateness of the ‘whale scale’ analytical technique for describing the prey field experienced by these large predators. Describing skewed data using the lognormal parameters (geomean and GSD) has the additional advantage of being less sensitive to outliers in the data, and summarizing acoustic data into spatially determined cells has the advantage of matching the spatial scale of collection with the spatial scale experienced by the predator under study.

In comparing the prey fields in super-group and non-super-group regions, we found that prey density was generally higher in super-group than in non-super-group regions. On 10 of 11 observation days (Table S3; Figure 5), geomean prey density at the whale scale ( $\overline{LN B_{WS}}$ ) was higher near super-groups than near foraging whales not in super-groups ( $p < 0.001$  in both environments): blue whale gulps in super-groups averaged  $1.5 \cdot 1.6 \text{ kg/m}^3$  ( $-47.5 \pm 2.2 \text{ dB}$ ) while gulps in non-super-groups averaged  $1.2 \cdot 1.8 \text{ kg/m}^3$  ( $-48.5 \pm 2.6 \text{ dB}$ ), and humpback whale gulps in super-groups averaged  $0.49 \cdot 2.0 \text{ kg/m}^3$  ( $-50.7 \pm 3.0 \text{ dB}$ ) while non-super-group gulps averaged  $0.31 \cdot 2.1 \text{ kg/m}^3$  ( $-52.7 \pm 3.3 \text{ dB}$ ). In 3 of 11 days, prey density was lower near super-groups if prey was described using whole patch means (further discussed below). Patches were additionally substantially and significantly thicker near super-groups in all cases (mean in South Africa:  $22 \pm 14$  m vs.  $8 \pm 9$  m, mean in Monterey:  $33 \pm 27$  m vs.  $15 \pm 15$  m, Figure 5; Table S3).

The GSD of gulps at the mean whale scale was not significantly different between super-group and non-super-group patches on any given day (Table S3). In 9 of 10 cases, the mean gulp at the mean informed whale scale (i.e. the mean gulp within the denser half of dive-sized cells) was significantly higher in super-groups, and in all

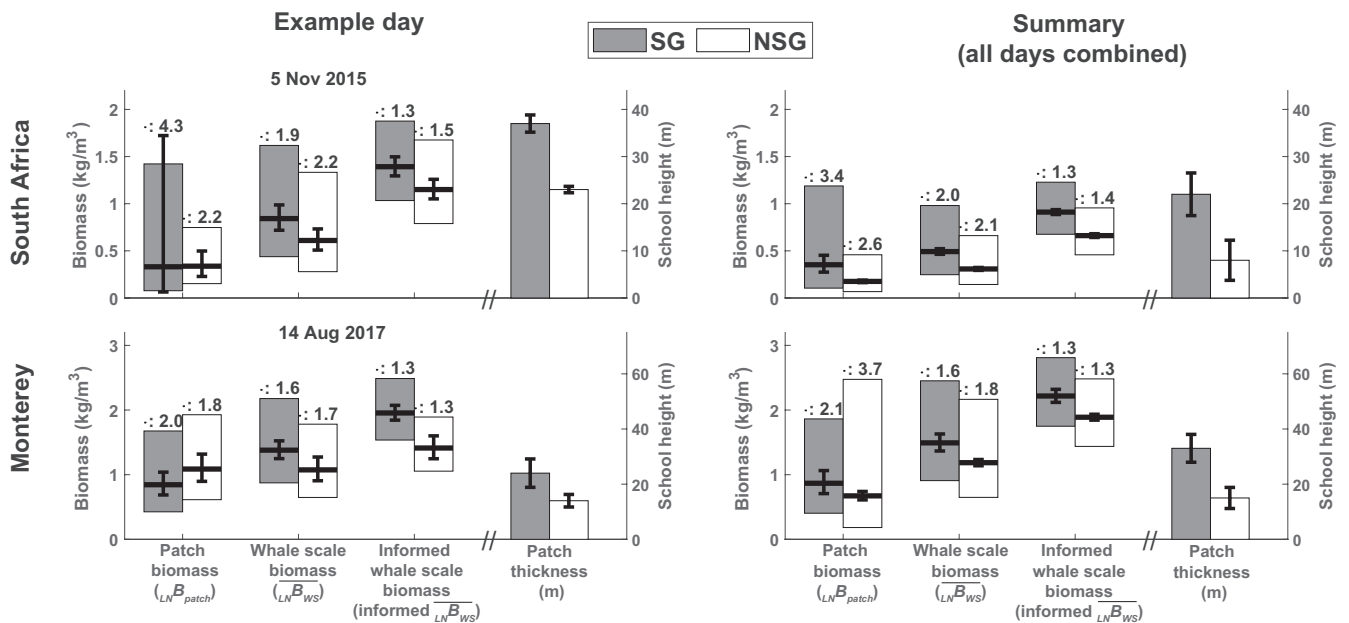


**FIGURE 5** Summary prey data from an example day and in aggregate for both South Africa and Monterey. Summary data for all days are displayed in Table S3. Symbol definitions in Table 3, SG = super-group, NSG = non-super-group. Prey patch geometric means are the thick horizontal bars, and the shaded bars represent the GSD with the multiplicative factor listed above each bar. Error bars around the geometric means are the 95% confidence intervals (calculated in acoustic units and converted to biomass). Patch thickness error bars are 95% confidence intervals

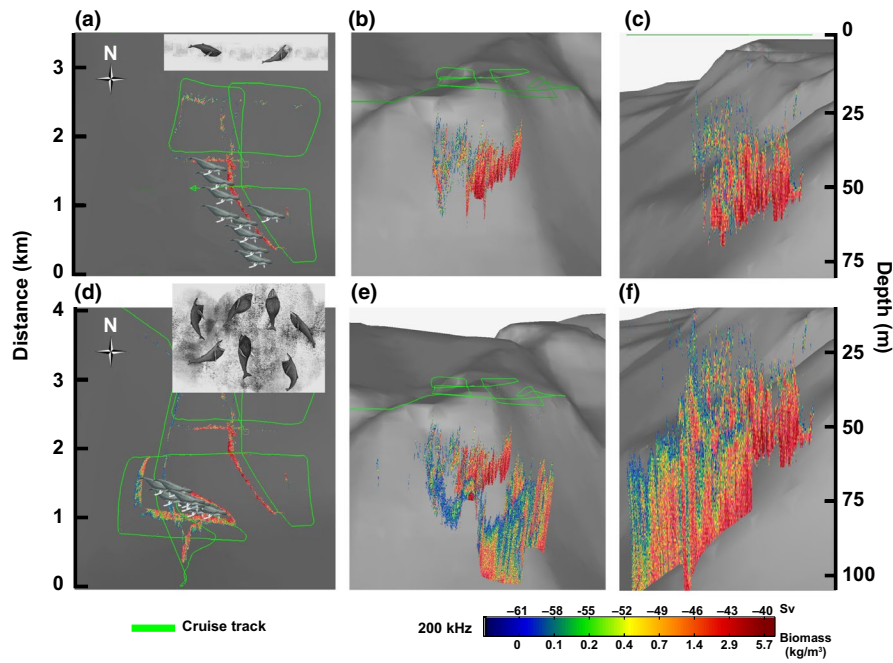


**FIGURE 6** 3D view of super-group-associated prey patch on 5 November 2015 in South Africa (the southernmost group in Figure 1). These are the same data from which Figure 4 was created. (a–c) Prey and whales spread out before super-group formation (prey data shown until 17:00 local time). (a) Overhead view. (b) Oblique view (from the northwest), highlighting the prey in relation to submarine canyon bathymetry. (c) Side-on view, looking from the south. (d–f) Same views now including super-group-associated data when 150–200 whales converged into a region ~200 m on a side at ~17:00. Bad weather on this day precluded suction-cup tag deployment. Whale illustrations by Alex Boersma. Bathymetry courtesy of the South Africa Navy Hydrographic Office. Data plotted in Echoview v10 using a 50× vertical exaggeration

cases the *SD* of gulp density at the mean informed whale scale was 0.1–0.6 dB lower in super-groups than non-super-groups.

Prey conditions in the same region both before and during super-group formation were observed just once in South Africa on 5 November 2015 (Figures 4 and 6). In that case, 150–200 whales were spread out along a shelf break before coming together into a single aggregation (Figure 6). Prey density in patch averages was not significantly different before or during super-group formation ( $p > 0.9$ , Figure 5). However, the geomean of gulps at the mean whale scale was 38% higher ( $p = 0.010$ ) in super-group-associated patches and was 21% higher at the mean informed whale scale ( $p = 0.002$ ). Additionally, mean patch thickness was estimated to be 14 m larger in super-groups ( $p < 0.001$ ), and gulp GSD at both the whale scale and the informed whale scale was smaller in super-groups, though only significantly so at the informed whale scale (Figure 5; Table S3).

In Monterey Bay, the blue whale super-group on 14 August 2017 demonstrated a similar pattern as the 5 November 2015 humpback whale super-group (Figure 5). While the geomean of patch biomass was smaller (but not significantly different) in the prey field near the observed super-group, geomean gulp biomass at the mean whale scale and the mean informed whale scale were both significantly and substantially higher (Figure 5; Table S3), and patch thickness and gulp GSD at the informed whale scale were significantly higher and lower respectively ( $p < 0.001$  in both cases, Table S3). While the super-group associated-patch on 16 August 2017 had slightly higher

geomean biomass at both the whale scale and in patches, results were non-significant (Table S3). Instead, prey around this super-group was characterized by a 2.5-fold increase in patch thickness as well as both a significant increase in geomean gulp biomass density and significant reduction in gulp GSD at the informed whale scale (Table S3).

Patches near super-groups thus had more available biomass on average than patches near whales not in super-groups. In both environments, better quality of super-group patches was indicated by higher geomean gulp density, thicker patches and indications that the prey at the informed whale scale (the denser half of the prey in each dive-sized cell) was more uniform in distribution (i.e. displayed smaller variance).

## 4 | DISCUSSION

Our results suggest that the formation of super-groups of two species of rorqual whales was largely influenced by high-quality foraging conditions. Gulp-sized cells analysed at the whale scale had higher geomean biomass and lower variability within prey patches associated with super-groups of humpback and blue whales, and whales within super-groups demonstrated higher feeding rates than more dispersed individuals. Furthermore, characterizing the intra-patch distribution of krill biomass appears to offer an explanation for the higher feeding rates observed in super-groups. Specifically, we found that super-groups were strongly associated with patches

characterized by high geomeans and low GSD of biomass, particularly in the densest half of gulps within dive-sized cells (the informed whale scale). Higher geomeans imply that even a naïvely foraging whale would benefit from increased energy intake at each feeding event, and a lower GSD (when paired with a high geomean) implies that a greater proportion of gulp-sized parcels would be of sufficient quality to feed (i.e. a greater proportion of gulps were above a threshold at which it would be beneficial to feed), enabling the observed increase in lunge-feeding events per unit time by decreasing search time. The match of predator behaviour (increased feeding rates) with our findings of higher density with less variance in cells the size of what a predator will experience on a foraging dive additionally supports the whale-scale level of analysis.

In ecological models of foraging in patchy environments, patch quality is often assessed as the overall intake (per unit time) enabled by an ecosystem (Giraldeau & Caraco, 2000). To improve the efficacy of such models, the intake rate parameter,  $\lambda$ , could further be decomposed into two component parts: 1) the energetic quality of each captured prey parcel and 2) the rate at which prey are captured. In rorqual whale foraging systems, these quantities are represented by the mean biomass density in each gulp ( $\lambda_p$ ) and the lunge rate per unit time ( $\lambda_f$ ), respectively, such that  $\lambda = \lambda_p \times \lambda_f$ . We found that prey patches associated with super-groups not only had 40%–50% more biomass in the median (geomean) gulp than patches not associated with super-groups, implying higher  $\lambda_p$ , but also had smaller GSD. The small GSD implied that prey was of more uniform quality proximal to super-groups, making it easier for whales to maximize consumption without spending time between lunges searching for the best nearby parcel. This reduction in search time likely facilitated the observed increases in super-group  $\lambda_f$  by decreasing the inter-lunge interval as well as the spatial distance travelled between lunges (Table 2). Indeed, the reported super-group feeding rates in both study areas (humpback whales:  $55 \pm 15$  lunges/hr, blue whales:  $24 \pm 2.9$  lunges/hr, Table 2) are comparable to the highest reported rates for whales in other studies: Goldbogen et al. (2008) report that one tagged humpback whale fed at a rate of 45 lunges/hr over 8 hr, Owen et al. (2017) report humpback feeding rates of 49 lunges/hr, while Southall et al. (2019) report blue whale feeding rates over 10-min bins that range from 5 to 30 lunges/hr when foraging, with mean rates typically <20 lunges/hr and max rates over foraging bout-comparable time-scales of approximately 25 lunges/hr. The high rates of foraging in super-groups suggest that these whales are feeding at rates close to their biomechanical limits.

The analysis of prey at the nested scales we describe is particularly well-suited for describing prey conditions available to krill-feeding rorqual whales because their foraging style utilizes characteristics of both filter-feeding, where energy cost per foraging event is independent of the quality of the prey, and raptorial feeding in which prey (i.e. in bulk patches) are engulfed in discrete units. The combination of these feeding modes distinguishes rorquals from right whales *Eubalaena glacialis*, whale sharks *Rhincodon typus* and other continuous ram filtration feeders. From our meta-analysis of data from 45 blue whales and 21 humpback whales that

lunged multiple times per dive and for which georeferenced tracks could be calculated, we found that those two species traverse an average of  $177 \pm 51$  and  $73 \pm 34$  horizontal metres between lunges and average  $4.1 \pm 1.4$  and  $5.2 \pm 2.3$  lunges per dive, respectively, yet the distance travelled for one lunge is only the length of the buccal cavity (12.8 and 6.0 m, respectively, for a 22.5 m blue whale and 10.5 m humpback whale). Right whales, approximately the same length as humpback whales, are continuous ram filtration filters that filter an average of  $670 \text{ m}^3$  of water on every dive (van der Hoop et al., 2019). At  $14 \text{ m}^3$  of water engulfed per lunge (Kahane-Rapport & Goldbogen, 2018), a humpback whale would have to lunge 48 times per dive (an order of magnitude more than their average) to filter an equivalent volume. These factors, combined with the ability to feed on more manoeuvrable prey enabled by high-speed, raptorial approaches (Cade et al., 2020), imply that rorqual whales may be energetically required to make active choices regarding what patch and what part of a patch to feed on, further supporting analysis at the informed whale scale.

Matching the spatial scale of analysis to the scale of the event under study is particularly critical in patchy environments (Benoit-Bird et al., 2013; Levin, 1992). Although the sensory mechanisms by which rorqual whales determine patch quality in the environment are currently unknown, insights into the process can be gleaned by proposing and examining potential behavioural algorithms used by whales to maximize their energy intake (Hein et al., 2020). Prior work has proposed that baleen whales initiate foraging when prey is available above a certain density (Cotté & Simard, 2005; Feyrer & Duffus, 2015; Hazen et al., 2009; Kirchner et al., 2018; Mayo & Marx, 1990). Our findings extend these ideas by suggesting that the density and distribution of encountered prey is a better indicator of where whales forage than overall patch or regional abundance. Future work may be able to refine this general principle into a prediction for a behavioural algorithm that would describe under what conditions a whale would give up foraging in one environment to take advantage of an environment it perceives as more favourable.

Better matching the scale of prey distribution to the scale of predator foraging effort could also be used to better predict overall intake rates ( $\lambda$ ). Considering that super-groups of two species of whales aggregated in regions with less variability in the densest half of the cell, and given that rorquals are likely not feeding indiscriminately, we suggest that the actual prey consumed by foraging rorqual whales would likely be reflected by the biomass of prey available at the whale scale as a lower bound, but be even better reflected by analysis at the informed whale scale, and we include suggestions for the calculation of these bounds in Appendix S1. Additional studies to quantify a more precise threshold for the informed whale scale could eventually shed light on how rorquals maximize their foraging efficiency in a given environment.

Although humpback and blue whale super-groups have only been recently described, abnormally large densities of krill do not appear to be a new phenomenon. Nicol et al. (1987) report surface swarms of *E. lucens* near our study area in South Africa of up to  $35 \text{ kg/m}^3$ . The historical record of super-groups (Bruce, 1915) followed by a

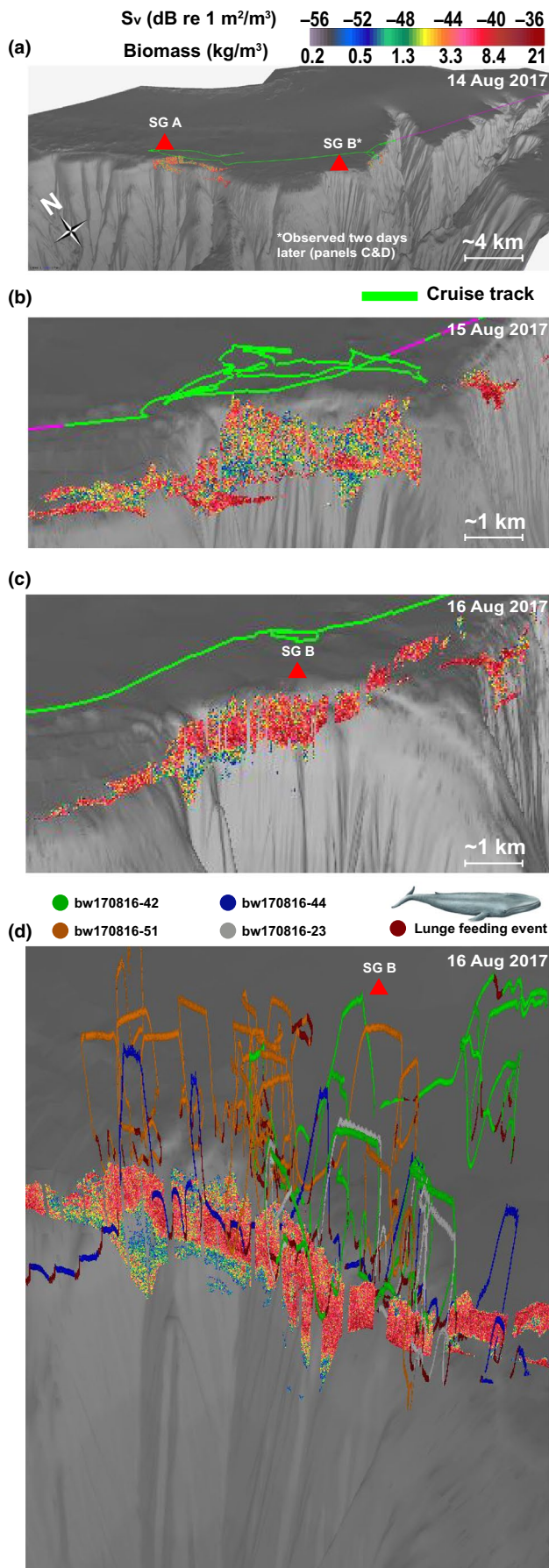


**FIGURE 7** 3D view of super-group (SG) associated prey patches in Monterey Bay, CA, USA. (a) Overall layout of the north Monterey Canyon edge with prey data near SG A on 14 August 2017. (b) Zoomed-in plot of the SG B location, but the day before the SG was noticed. There were scattered blue whales feeding in this area, but it is noticeable how much less uniform and diffuse the high-quality parts of this large patch are. (c) Zoomed-in plot of the SG B associated patch on 16 August 2017. (d) View from the southeast of the same patch, overlain with tracks from the four tagged whales feeding within SG B. Data plotted in Echoview v10 using a 10x vertical exaggeration

lack of observed occurrences during periods of low cetacean abundance combined with consistent aggregations of krill suggest that rorqual whale super-groups were once a more common occurrence. Given the 20%–60% increase in geomean prey density we found in super-groups and the concurrent 33%–45% increase in feeding rates compared to non-super-group environments, it is likely that super-groups were once an important part of rorqual whale foraging ecology before anthropogenic hunting removed more than three million whales globally (Rocha et al., 2014). It is plausible, therefore, that recovering populations benefit from a positive feedback loop whereby increasing population sizes increase the likelihood of discovering extensive but ephemeral (Figure 7) patches since concentrations of calling whales, even if calling is not directly related to patch quality or extent, could serve as a signpost for wanderers about the location of ephemeral, high-quality foraging grounds (Wilson et al., 2018). This socially mediated information exchange would decrease the search time of individuals who might not otherwise find the highest quality regions within a foraging ground (Hein & Martin, 2020; LaScala-Gruenewald et al., 2019).

The spatial collocation of the observed super-group-associated patches with bathymetric features, including small scale (1–5 km wide) canyons that incise typical rorqual foraging habitat regions off the edges of continental shelves (Figures 1, 6 and 7), suggests that the two environments in our study may have a specific proclivity to support large, dense prey patches due to the interaction of bathymetry and local oceanographic process that have been shown to aggregate zooplankton (e.g. Benoit-Bird et al., 2019; Santora et al., 2018). Future work examining the spatiotemporal links between mesoscale oceanographic processes, local bathymetry and temporally transient prey conditions may better help explain how these large predators effectively exploit prey in spatially and temporally complex habitats.

It was not until relatively recently in the fossil record (5–7 Ma) that baleen whales developed gigantic body sizes (>10 m), and it is likely that this large change came about in concert with oceanic conditions that favoured annually consistent upwelling zones that brought nutrient-rich water to the surface in specific areas, creating natural aggregation areas (Slater et al., 2017). Locating and exploiting these prey hotspots is essential to the foraging strategy of rorqual whales, and we found that differentiating the highest quality prey areas (as characterized by high geometric means and low GSD) from merely good prey areas can result in a doubling of intake rates

( $\lambda$ ) when increased feeding rates ( $\lambda_f$ ) are combined with increased prey density ( $\lambda_p$ ). We have described two disparate environments in which predator patchiness—indicated by temporally transient and spatially limited super-group formation—is driven by prey patchiness, and we utilize predator-specific prey density metrics to characterize high-quality whale habitat. Our results suggest that foregoing local foraging within good prey environments in favour of traversing to great prey environments where conspecifics are aggregating may be an evolutionarily stable strategy when such prey patches are extensive and ephemeral, and future research may reveal the specific social drivers that cue whales into the locations of these high-quality foraging hotspots.

## ACKNOWLEDGEMENTS

The authors thank Duke Marine Robotics and Remote Sensing for UAV images, Tamara Goldbogen for data transfer, John Ryan for contributions related to the spatial locations of super-groups, and the crews of the RV FRS Ellen Khuzwayo and the Moss Landing Marine Labs based RV John Martin. All cetacean data collected under NMFS permits 16111, 20430 and South African permits RES2015/DEA and RES2016/DEA. All procedures were conducted under institutional IACUC protocols. This work funded with NSF IOS grant #1656691, ONR YIP grant #N000141612477, Stanford University's Terman and Bass Fellowships, and funding from the South African Department of the Environment, Forestry and Fisheries. Monterey bathymetric data provided by MBARI and NOAA's National Centers for Environmental Information. South African bathymetric data provided by the South African Navy Hydrographic Office.

## AUTHORS' CONTRIBUTIONS

D.E.C., S.M.S., K.P.F., J.C., A.S.F., E.L.H. and J.A.G. drove investigation; J.D.W. calculated TS of *E. lucens* and *T. spinifera*; D.E.C., J.F. and J.A.G. prepared hydroacoustic data for processing; D.E.C. and S.R.K.-R. analysed feeding rates from tag data; D.E.C., S.M.S., K.P.F., D.K., S.M., M.M., M.G.O., C.W., J.C., A.S.F., J.A.F., E.L.H., S.R.K.-R., W.K.O. and J.A.G. collected field data; D.E.C. processed the hydroacoustic and tag data, performed statistical analyses and led the writing of the manuscript. All the authors contributed substantially to revisions and gave final approval for publication.

## DATA AVAILABILITY STATEMENT

Prey and tag data have been deposited at Stanford University's digital repository: <https://purl.stanford.edu/rq794kc6747>. Monterey Bay bathymetric NAVD88 data at 1/3 arc-second resolution used for Figure 7 was downloaded from [www.ncei.noaa.gov](http://www.ncei.noaa.gov).

## ORCID

David E. Cade  <https://orcid.org/0000-0003-3641-1242>  
 S. Mduduzi Seakamela  <https://orcid.org/0000-0002-7873-208X>  
 Ken P. Findlay  <https://orcid.org/0000-0001-7154-8805>  
 Shirel R. Kahane-Rapport  <https://orcid.org/0000-0002-5208-1100>

Joseph D. Warren  <https://orcid.org/0000-0001-6920-1554>  
 James A. Fahlbusch  <https://orcid.org/0000-0001-9275-013X>  
 Ari S. Friedlaender  <https://orcid.org/0000-0002-2822-233X>  
 Elliott L. Hazen  <https://orcid.org/0000-0002-0412-7178>  
 Deon Kotze  <https://orcid.org/0000-0002-2136-9056>  
 Steven McCue  <https://orcid.org/0000-0001-9601-0067>  
 Michael Mejer  <https://orcid.org/0000-0002-9486-5448>  
 William K. Oestreich  <https://orcid.org/0000-0002-0137-5053>  
 Machiel G. Oudejans  <https://orcid.org/0000-0003-4212-6712>  
 Jeremy A. Goldbogen  <https://orcid.org/0000-0002-4170-7294>

## REFERENCES

- Abrahms, B., Hazen, E. L., Aikens, E. O., Savoca, M. S., Goldbogen, J. A., Bograd, S. J., Jacox, M. G., Irvine, L. M., Palacios, D. M., & Mate, B. R. (2019). Memory and resource tracking drive blue whale migrations. *Proceedings of the National Academy of Sciences of the United States of America*, 116, 5582–5587. <https://doi.org/10.1073/pnas.1819031116>
- Anand, M., & Li, B. (2001). Spatiotemporal dynamics in a transition zone: Patchiness, scale, and an emergent property. *Community Ecology*, 2, 161–169. <https://doi.org/10.1556/ComEc.2.2001.2.3>
- Barange, M. (1994). Acoustic identification, classification and structure of biological patchiness on the edge of the Agulhas Bank and its relation to frontal features. *South African Journal of Marine Science*, 14, 333–347. <https://doi.org/10.2989/025776194784286969>
- Barnes, H. (1952). The use of transformations in marine biological statistics. *ICES Journal of Marine Science*, 18, 61–71. <https://doi.org/10.1093/icesjms/18.1.61>
- Baumgartner, M. F., & Mate, B. R. (2003). Summertime foraging ecology of North Atlantic right whales. *Marine Ecology Progress Series*, 264, 123–135. <https://doi.org/10.3354/meps264123>
- Bennett, A. F., & Denman, K. L. (1985). Phytoplankton patchiness: Inferences from particle statistics. *Journal of Marine Research*, 43, 307–335. <https://doi.org/10.1357/002224085788438711>
- Benoit-Bird, K. J., Battaile, B. C., Heppell, S. A., Hoover, B., Irons, D., Jones, N., Kuletz, K. J., Nordstrom, C. A., Paredes, R., Suryan, R. M., Waluk, C. M., & Trites, A. W. (2013). Prey patch patterns predict habitat use by top marine predators with diverse foraging strategies. *PLoS ONE*, 8, e53348. <https://doi.org/10.1371/journal.pone.0053348>
- Benoit-Bird, K. J., Moline, M. A., & Southall, B. L. (2017). Prey in oceanic sound scattering layers organize to get a little help from their friends. *Limnology and Oceanography*, 62, 2788–2798. <https://doi.org/10.1002/lno.10606>
- Benoit-Bird, K. J., Waluk, C. M., & Ryan, J. P. (2019). Forage species swarm in response to coastal upwelling. *Geophysical Research Letters*, 46, 1537–1546. <https://doi.org/10.1029/2018GL081603>
- Benson, S. R., Croll, D. A., Marinovic, B. B., Chavez, F. P., & Harvey, J. T. (2002). Changes in the cetacean assemblage of a coastal upwelling ecosystem during El Niño 1997–98 and La Niña 1999. *Progress in Oceanography*, 54, 279–291. [https://doi.org/10.1016/S0079-6611\(02\)00054-X](https://doi.org/10.1016/S0079-6611(02)00054-X)
- Bruce, W. (1915). Some observations on Antarctic cetacea. *Scottish National Antarctic Expedition*, 4, 491–505.
- Cade, D. E., Carey, N., Domenici, P., Potvin, J., & Goldbogen, J. A. (2020). Predator-informed looming stimulus experiments reveal how large filter feeding whales capture highly maneuverable forage fish. *Proceedings of the National Academy of Sciences of the United States of America*, 117, 472–478. <https://doi.org/10.1073/pnas.1911099116>
- Cade, D. E., Friedlaender, A. S., Calambokidis, J., & Goldbogen, J. A. (2016). Kinematic diversity in rorqual whale feeding mechanisms. *Current Biology*, 26, 2617–2624. <https://doi.org/10.1016/j.cub.2016.07.037>
- Campbell, J. W. (1995). The lognormal distribution as a model for bio-optical variability in the sea. *Journal of Geophysical Research: Oceans*, 100, 13237–13254. <https://doi.org/10.1029/95JC00458>

- Chave, J. (2013). The problem of pattern and scale in ecology: What have we learned in 20 years? *Ecology Letters*, 16, 4–16.
- Coetzee, J. (2000). Use of a shoal analysis and patch estimation system (SHAPES) to characterise sardine schools. *Aquatic Living Resources*, 13, 1–10. [https://doi.org/10.1016/S0990-7440\(00\)00139-X](https://doi.org/10.1016/S0990-7440(00)00139-X)
- Cotté, C., & Simard, Y. (2005). Formation of dense krill patches under tidal forcing at whale feeding hot spots in the St. Lawrence Estuary. *Marine Ecology Progress Series*, 288, 199–210. <https://doi.org/10.3354/meps288199>
- Cox, M. J., Demer, D. A., Warren, J. D., Cutter, G. R., & Brierley, A. S. (2009). Multibeam echosounder observations reveal interactions between Antarctic krill and air-breathing predators. *Marine Ecology Progress Series*, 378, 199–209. <https://doi.org/10.3354/meps07795>
- Croll, D. A., Tershy, B. R., Hewitt, R. P., Demer, D. A., Fiedler, P. C., Smith, S. E., Armstrong, W., Popp, J. M., Kiekhefer, T., & Lopez, V. R. (1998). An integrated approach to the foraging ecology of marine birds and mammals. *Deep Sea Research Part II: Topical Studies in Oceanography*, 45, 1353–1371.
- Dennis, B., & Patil, G. P. (1987). Applications in ecology. In E. L. Crow & K. Shimizu (Eds.), *Lognormal distributions* (pp. 303–330). Marcel Dekker.
- Feyrer, L. J., & Duffus, D. A. (2015). Threshold foraging by gray whales in response to fine scale variations in mysid density. *Marine Mammal Science*, 31, 560–578. <https://doi.org/10.1111/mms.12178>
- Findlay, K. P., Seakamela, S. M., Meyer, M. A., Kirkman, S. P., Barendse, J., Cade, D. E., Hurwitz, D., Kennedy, A., Kotze, P. G. H., McCue, S. A., Thornton, M., Vargas-Fonseca, O. A., & Wilke, C. G. (2017). Humpback whale 'super-groups' – A novel low-latitude feeding behaviour of Southern Hemisphere humpback whales (*Megaptera novaeangliae*) in the Benguela upwelling system. *PLoS ONE*, 12, e0172002. <https://doi.org/10.1371/journal.pone.0172002>
- Fossette, S., Abrahms, B., Hazen, E. L., Bograd, S. J., Zilliacus, K. M., Calambokidis, J., Burrows, J. A., Goldbogen, J. A., Harvey, J. T., Marinovic, B., Tershy, B. R., & Croll, D. A. (2017). Resource partitioning facilitates coexistence in sympatric cetaceans in the California Current. *Ecology and Evolution*, 7, 9085–9097. <https://doi.org/10.1002/ece3.3409>
- Giraldeau, L.-A., & Caraco, T. (2000). Ch 8- social patch and prey models. In *Social foraging theory*. (pp. 205–226). Princeton University Press.
- Goldbogen, J. A., Cade, D. E., Calambokidis, J., Friedlaender, A. S., Potvin, J., Segre, P. S., & Werth, A. J. (2017). How baleen whales feed: The biomechanics of engulfment and filtration. *Annual Review of Marine Science*, 9, 1–20. <https://doi.org/10.1146/annurev-marine-122414-033905>
- Goldbogen, J. A., Cade, D. E., Wisniewska, D. M., Potvin, J., Segre, P. S., Savoca, M. S., Hazen, E. L., Czapan斯基, M. F., Kahane-Rapport, S. R., DeRuiter, S. L., Gero, S., Tønnesen, P., Gough, W. T., Hanson, M. B., Holt, M., Jensen, F. H., Simon, M., Stimpert, A. K., Arranz, P., ... Pyenson, N. D. (2019). Why whales are big but not bigger: Physiological drivers and ecological limits in the age of ocean giants. *Science*, 366, 1367–1372. <https://doi.org/10.1126/science.aax9044>
- Goldbogen, J. A., Calambokidis, J., Croll, D. A., Harvey, J. T., Newton, K. M., Oleson, E. M., Schorr, G., & Shadwick, R. E. (2008). Foraging behavior of humpback whales: Kinematic and respiratory patterns suggest a high cost for a lunge. *Journal of Experimental Biology*, 211, 3712–3719. <https://doi.org/10.1242/jeb.023366>
- Goldbogen, J. A., Calambokidis, J., Croll, D. A., McKenna, M. F., Oleson, E., Potvin, J., Pyenson, N. D., Schorr, G., Shadwick, R. E., & Tershy, B. R. (2012). Scaling of lunge-feeding performance in rorqual whales: Mass-specific energy expenditure increases with body size and progressively limits diving capacity. *Functional Ecology*, 26, 216–226. <https://doi.org/10.1111/j.1365-2435.2011.01905.x>
- Gordon, D. M. (2014). The ecology of collective behavior. *PLoS Biology*, 12, e1001805. <https://doi.org/10.1371/journal.pbio.1001805>
- Guilpin, M., Lesage, V., McQuinn, I., Goldbogen, J. A., Potvin, J., Jeanniard-du-Dot, T., Doniol-Valcroze, T., Michaud, R., Moisan, M., & Winkler, G. (2019). Foraging energetics and prey density requirements of western North Atlantic blue whales in the Estuary and Gulf of St. Lawrence, Canada. *Marine Ecology Progress Series*, 625, 205–223. <https://doi.org/10.3354/meps13043>
- Hazen, E. L., Friedlaender, A. S., & Goldbogen, J. A. (2015). Blue whale (*Balaenoptera musculus*) optimize foraging efficiency by balancing oxygen use and energy gain as a function of prey density. *Science Advances*, 1, e1500469.
- Hazen, E. L., Friedlaender, A. S., Thompson, M. A., Ware, C. R., Weinrich, M. T., Halpin, P. N., & Wiley, D. N. (2009). Fine-scale prey aggregations and foraging ecology of humpback whales *Megaptera novaeangliae*. *Marine Ecology Progress Series*, 395, 75–89. <https://doi.org/10.3354/meps08108>
- Hein, A. M., Altshuler, D. L., Cade, D. E., Liao, J. C., Martin, B. T., & Taylor, G. K. (2020). An algorithmic approach to natural behavior. *Current Biology*, 30, R663–R667.
- Hein, A. M., & Martin, B. T. (2020). Information limitation and the dynamics of coupled ecological systems. *Nature Ecology & Evolution*, 4, 82–90. <https://doi.org/10.1038/s41559-019-1008-x>
- Jaquet, N. (1996). *Distribution and spatial organization of groups of sperm whales in relation to biological and environmental factors in the South Pacific* (PhD thesis). Dalhousie University.
- Jarvis, T., Kelly, N., Kawaguchi, S., van Wijk, E., & Nicol, S. (2010). Acoustic characterisation of the broad-scale distribution and abundance of Antarctic krill (*Euphausia superba*) off East Antarctica (30–80 E) in January–March 2006. *Deep Sea Research Part II: Topical Studies in Oceanography*, 57, 916–933. <https://doi.org/10.1016/j.jdsr.2008.06.013>
- Jurasz, C. M., & Jurasz, V. P. (1979). Feeding modes of the humpback whale (*Megaptera Novaeangliae*) in southeast Alaska. *Scientific Reporting of Whales Research Institute*, 31, 69–83.
- Kaartvedt, S., Røstad, A., Fiksen, Ø., Melle, W., Torgersen, T., Breien, M. T., & Kleivjer, T. A. (2005). Piscivorous fish patrol krill swarms. *Marine Ecology Progress Series*, 299, 1–5. <https://doi.org/10.3354/meps299001>
- Kahane-Rapport, S. R., & Goldbogen, J. A. (2018). Allometric scaling of morphology and engulfment capacity in rorqual whales. *Journal of Morphology*, 1–13. <https://doi.org/10.1002/jmor.20846>
- Kirchner, T., Wiley, D. N., Hazen, E. L., Parks, S. E., Torres, L. G., & Friedlaender, A. S. (2018). Hierarchical foraging movement of humpback whales relative to the structure of their prey. *Marine Ecology Progress Series*, 607, 237–250. <https://doi.org/10.3354/meps12789>
- LaScala-Gruenewald, D. E., Mehta, R. S., Liu, Y., & Denny, M. W. (2019). Sensory perception plays a larger role in foraging efficiency than heavy-tailed movement strategies. *Ecological Modelling*, 404, 69–82. <https://doi.org/10.1016/j.ecolmodel.2019.02.015>
- Leibniz, G. (1684). A new method for maxima and minima as well as tangents, which is neither impeded by fractional nor irrational quantities, and a remarkable type of calculus for them (translation). In D. J. Struik (Ed.), *A source book in mathematics, 1200–1800* (pp. 271–281). Harvard University Press.
- Levin, S. A. (1992). The problem of pattern and scale in ecology: The Robert H. MacArthur award lecture. *Ecology*, 73, 1943–1967. <https://doi.org/10.2307/1941447>
- MacLennan, D. N., Fernandes, P. G., & Dalen, J. (2002). A consistent approach to definitions and symbols in fisheries acoustics. *ICES Journal of Marine Science*, 59, 365–369. <https://doi.org/10.1006/jmsc.2001.1158>
- Magurran, A. E., & Henderson, P. A. (2003). Explaining the excess of rare species in natural species abundance distributions. *Nature*, 422, 714–716. <https://doi.org/10.1038/nature01547>
- Mann, J. (2000). Unraveling the dynamics of social life. In J. Mann, R. C. Connor, P. Tyack, & H. Whitehead (Eds.), *Cetacean societies: Field studies of dolphins and whales* (pp. 45–64). University of Chicago Press.

- Mastick, N. (2016). *The effect of group size on individual roles and the potential for cooperation in group bubble-net feeding humpback whales (Megaptera novaeangliae)* (M.S. thesis). Oregon State University.
- Mayo, C. A., & Marx, M. K. (1990). Surface foraging behaviour of the North Atlantic right whale, *Eubalaena glacialis*, and associated zooplankton characteristics. *Canadian Journal of Zoology*, *68*, 2214–2220.
- Nickels, C. F., Sala, L. M., & Ohman, M. D. (2019). The euphausiid prey field for blue whales around a steep bathymetric feature in the southern California current system. *Limnology and Oceanography*, *64*, 390–405. <https://doi.org/10.1002/lno.11047>
- Nicol, S., James, A., & Pitcher, G. (1987). A first record of daytime surface swarming by *Euphausia lucens* in the Southern Benguela region. *Marine Biology*, *94*, 7–10. <https://doi.org/10.1007/BF00392893>
- Nowacek, D. P., Friedlaender, A. S., Halpin, P. N., Hazen, E. L., Johnston, D. W., Read, A. J., Espinasse, B., Zhou, M., & Zhu, Y. (2011). Super-aggregations of krill and humpback whales in Wilhelmina Bay, Antarctic Peninsula. *PLoS ONE*, *6*, e19173. <https://doi.org/10.1371/journal.pone.0019173>
- Owen, K., Kavanagh, A. S., Warren, J. D., Noad, M. J., Donnelly, D., Goldizen, A. W., & Dunlop, R. A. (2017). Potential energy gain by whales outside of the Antarctic: Prey preferences and consumption rates of migrating humpback whales (*Megaptera novaeangliae*). *Polar Biology*, *40*, 277–289. <https://doi.org/10.1007/s00300-016-1951-9>
- Pagel, M. D., Harvey, P. H., & Godfray, H. (1991). Species-abundance, biomass, and resource-use distributions. *The American Naturalist*, *138*, 836–850. <https://doi.org/10.1086/285255>
- Piatt, J. F., & Methven, D. A. (1992). Threshold foraging behavior of baleen whales. *Marine Ecology Progress Series*, *84*, 205–210. <https://doi.org/10.3354/meps084205>
- Pivorunas, A. (1979). The feeding mechanisms of baleen whales. *American Scientist*, *67*, 432–440.
- Preston, F. W. (1948). The commonness, and rarity, of species. *Ecology*, *29*, 254–283. <https://doi.org/10.2307/1930989>
- Preston, F. W. (1962). The canonical distribution of commonness and rarity: Part I. *Ecology*, *43*, 185–215. <https://doi.org/10.2307/1931976>
- Przybylski, A. K., Murayama, K., DeHaan, C. R., & Gladwell, V. (2013). Motivational, emotional, and behavioral correlates of fear of missing out. *Computers in Human Behavior*, *29*, 1841–1848. <https://doi.org/10.1016/j.chb.2013.02.014>
- Rocha, R. C., Clapham, P. J., & Ivashchenko, Y. V. (2014). Emptying the oceans: A summary of industrial whaling catches in the 20th century. *Marine Fisheries Review*, *76*, 37–48. <https://doi.org/10.7755/MFR.76.4.3>
- Santora, J. A., Zeno, R., Dorman, J. G., & Sydeman, W. J. (2018). Submarine canyons represent an essential habitat network for krill hotspots in a large marine ecosystem. *Scientific Reports*, *8*, 7579. <https://doi.org/10.1038/s41598-018-25742-9>
- Slater, G. J., Goldbogen, J. A., & Pyenson, N. D. (2017). Independent evolution of baleen whale gigantism linked to Plio-Pleistocene ocean dynamics. *Proceedings of the Royal Society B*, *284*, 20170546.
- Southall, B. L., DeRuiter, S. L., Friedlaender, A., Stimpert, A. K., Goldbogen, J. A., Hazen, E., Casey, C., Fregosi, S., Cade, D. E., & Allen, A. N. (2019). Behavioral responses of individual blue whales (*Balaenoptera musculus*) to mid-frequency military sonar. *Journal of Experimental Biology*, *222*. <https://doi.org/10.1242/jeb.190637>
- Stephens, D. W., & Krebs, J. R. (1986). *Foraging theory*. Princeton University Press.
- van der Hoop, J., Nousek-McGregor, A., Nowacek, D., Parks, S., Tyack, P., & Madsen, P. (2019). Foraging rates of ram-filtering North Atlantic right whales. *Functional Ecology*, *33*, 1290–1306. <https://doi.org/10.1111/1365-2435.13357>
- Watkins, J. L., & Murray, A. W. A. (1998). Layers of Antarctic krill, *Euphausia superba*: Are they just long krill swarms? *Marine Biology*, *131*, 237–247.
- White, G. C. (1978). Estimation of plant biomass from quadrat data using the lognormal distribution. *Journal of Range Management*, *118*–120. <https://doi.org/10.2307/3897657>
- Whitehead, H. (1983). Structure and stability of humpback whale groups off Newfoundland. *Canadian Journal of Zoology*, *61*, 1391–1397. <https://doi.org/10.1139/z83-186>
- Wiley, D. N., Ware, C., Bocconcelli, A., Cholewiak, D., Friedlaender, A., Thompson, M., & Weinrich, M. (2011). Underwater components of humpback whale bubble-net feeding behavior. *Behaviour*, *148*, 575–602.
- Wilson, R. P., Neate, A., Holton, M. D., Shepard, E. L., Scantlebury, D. M., Lambertucci, S. A., di Virgilio, A., Crooks, E., Mulvenna, C., & Marks, N. (2018). Luck in food finding affects individual performance and population trajectories. *Current Biology*, *28*, 3871–3877, e3875.

## SUPPORTING INFORMATION

Additional supporting information may be found online in the Supporting Information section.

**How to cite this article:** Cade DE, Seakamela SM, Findlay KP, et al. Predator-scale spatial analysis of intra-patch prey distribution reveals the energetic drivers of orca whale super-group formation. *Funct Ecol*. 2021;35:894–908. <https://doi.org/10.1111/1365-2435.13763>

# Predator-scale spatial analysis of intra-patch prey distribution reveals the energetic drivers of rorqual whale super-group formation

David E. Cade, S. Mduduzi Seakamela, Ken P. Findlay, Julie Fukunaga, Shirel R. Kahane-Rapport, Joseph D. Warren, John Calambokidis, James A. Fahlbusch, Ari S. Friedlaender, Elliott L. Hazen, Deon Kotze, Steven McCue, Michael Meÿer, William K. Oestreich, Machiel G. Oudejans, Christopher Wilke, Jeremy A. Goldbogen

## Supporting Information

This combined pdf file contains the following linked sections:

Appendix S1- Detailed methods

*Field methods*

*Foraging behavior*

*Feeding rate analysis*

*Prey data collection*

*Prey data processing*

*Distribution of resources*

*Additional test for acoustic artefacts*

*Estimating overall intake*

Figure S1- Distribution of gulp sized cells of acoustic energy and biomass for each day

Figure S2- Comparisons of bottom echo strength in adjacent regions of varying water column echos

Figure S3- Plots of  $S_a$  for each 200 kHz ping on 05 Nov 2015

Figure S4- Surface interval between foraging dives for blue whales and humpback whales tagged in multiple ecosystems

Table S1- Summary of data collected near super-groups

Table S2- Feeding parameters from tag data for individual whale

Table S3- Summary prey data from each day with super-group observations

Video S1- On animal video from humpback whales foraging within super-groups, high quality version available with deposited data at: <https://purl.stanford.edu/rq794kc6747>

Supplemental References

## Appendix S1- Detailed methods

### *Field methods*

Operations in South Africa were based on the RV FRS Ellen Khuzwayo and two small boats were launched to conduct tagging and observation work (additional details in Findlay *et al.* 2017). Monterey Bay operations were based on shore with daily excursions in the RV John Martin and two rigid hull inflatable boats (RHIBs); surveys were conducted along the shelf break until blue whales were found. Unlike in South Africa, super-groups were not targeted specifically but were encountered opportunistically and boats often conducted UAV (unoccupied aerial vehicles) and tagging operations around individual whales that were encountered. In both locations whales were approached in a 6 m RHIB and a 6 m pole was used to deploy suction cup attached video and 3D accelerometer tags manufactured by Customized Animal Tracking Solutions (CATS) (Cade *et al.* 2016). When super-groups were found or whales were tagged, the larger RV either conducted additional support operations (e.g. UAV work around tagged animals) or conducted acoustic surveys in a box pattern around tagged whales. All data used in this project were collected under NMFS permits 16111, 14809, and 20430 and South African permits RES2015/DEA and RES2016/DEA.

### *Foraging behavior*

Our analysis of behavior in super-groups consisted of 3D movement data from six tagged humpback whales and six tagged blue whales (Table S2). We deployed two CATS tags on humpback whales in super-group in 2015 as well as four additional tags on whales not in super-groups. One of these animals travelled south for the duration of the deployment (3.5 hrs) and did not feed so was excluded from analysis. In general, periods of super-group activity for humpback whales were directly observed from the surface (mean deployment duration:  $6.2 \pm 3.9$  hrs), however one of the non-super-group animals demonstrated localized, intensive feeding behavior at night and was observed in the morning in the vicinity of > 20 other whales, so this localized feeding bout was included in the super-group analysis. Additional

periods of super-group behavior in 2016 were also identified when direct tag video confirmation could be made of at least six animals feeding within an estimated five body lengths of the tagged whale (Fig 2). In 2016 we deployed six tags on super-group whales, though two were of short duration (<10 minutes) and one collected video but no data; these three were excluded.

We deployed four tags on blue whale in the two described super-groups, and also had two whales with tags on join the super-group on 16 Aug. With much longer deployments averaging  $9.5 \pm 10.8$  hrs during which whales were not observed for the duration of their deployments, periods of blue whale super-group behavior were identified as periods during which the whales were within a restricted region ( $\sim 1$  nm across) at the head of the canyon in which the super-group was observed.

#### *Feeding rate analysis*

Tag accelerometers for all whales were sampled at 40 or 400 Hz, magnetometers and gyroscopes at 40 or 50 Hz, and pressure, light, temperature and GPS at 10 Hz. All data were decimated to 10 Hz, tag orientation on the animal was corrected for, and animal orientation was calculated using custom-written scripts in Matlab 2014a (following Johnson & Tyack 2003; Cade *et al.* 2016). Animal speed for all deployments was determined using the amplitude of tag vibrations (Cade *et al.* 2018).

Rorqual whale feeding behavior is a constant optimization problem balancing resource acquisition at depth with oxygen acquisition at the surface (Hazen, Friedlaender & Goldbogen 2015). Stereotypical behavior consists of diving from the surface, lunge feeding one to ten times at depths ranging from the surface to  $> 300$  m, then surfacing for one to a dozen or more breaths and then diving to forage again. When this behavior repeats without a prolonged break it is known as a foraging bout. Lunge feeding on krill is highly stereotypical (Goldbogen *et al.* 2006; Cade *et al.* 2016) and individual lunges can be identified from the tag records as peaks in speed followed by rapid deceleration that corresponds to increases in dynamic body acceleration as well as changes in pitch, roll and heading associated with maneuvering (Simon, Johnson & Madsen 2012; Cade *et al.* 2016). Dives to  $> 5$  m were identified as feeding dives if they included at least one lunge. To determine the average duration of foraging bouts across these two species we analyzed

the largest published collection of cetacean bio-logging data from Goldbogen *et al.* (2019), which consisted of 112 feeding blue whales – 67 from Southern California (Cade *et al.* 2016; Southall *et al.* 2019) and 45 from Monterey Bay – and 42 krill-feeding humpback whales – 17 from the West Antarctic Peninsula, 9 from South Africa, 12 from Monterey Bay and 4 from WA inland waters. Foraging bouts were differentiated by examining the distributions of surface intervals between the end of a feeding dive and the start of the next dive (feeding or not). Surface interval for all whales demonstrated clear bi or multimodal distributions (Fig S4), so Gaussian curves were fit (using the `fitgmdist` function in Matlab 2014a, see Cade & Benoit-Bird 2014) and the first set of curves that best matched the shape of the distribution was selected. AIC and BIC continued to drop as the model complexity increased, but the change was < 5% each time and additional  $\mu$ s were outside the bulk of the data. The surface interval equivalent to the final  $\mu$  in the bulk of the data plus  $3\sigma$  was chosen as the value to separate feeding behavior into foraging bouts. Feeding dives separated by more than this inter-bout interval (5.5 minutes for both species) were considered to be part of separate foraging bouts. Feeding rates (lunges/hr within foraging bouts during super-group and non-super-group times) were determined for all whales by dividing the number of lunges by the total duration of all foraging bouts.

Other parameters analyzed, including inter-lunge interval (ILI), dive duration, lunges per dive and search area per lunge were determined on a dive-by-dive scale and averaged. Results in Table S2 are the mean and standard deviation (*SD*) for each super-group whale. ILI is the time (s) between the peak in speed (nearly equivalent to mouth opening time, Cade *et al.* 2016) from one lunge to the next peak in speed in the next lunge of that dive. Dive duration was the time from leaving the surface to reaching the surface for all dives > 5 m (calculated via `finddives.m` from `animaltags.org`). Search area between lunges was determined using the geo-referenced pseudotrack (Wilson *et al.* 2007) of the whale, calculated from whale speed, pitch and heading, and then distributing the resulting positional error between every two known positions. The set of spatial x and y coordinates (z was calculated but not used) of the whale between lunges was then used to find the two points that were furthest apart horizontally ( $p_1$  and  $p_2$ ). Additionally, the points furthest from the line segment  $\overline{p_1p_2}$  (one point above and one below) were identified and the distance from each

point to  $\overline{p_1 p_2}$  was calculated. Search area between each pair of lunges in a dive was then calculated as the length of  $\overline{p_1 p_2}$  multiplied by the sum of the distances of the two additional points from the line.

### *Prey data collection*

Acoustic backscatter data were collected only during daylight hours using Simrad EK60 or EK80 transceivers with split-beam 38 kHz and either 120 or 200 kHz transducers in both ecosystems. In South Africa, all three frequencies (EK60) were hull mounted on the RV Khuzwayo and transmitted pulses when in the vicinity of whales, but the 120 kHz transducer was only operable for 5 of the 15 sea days. All three transducers had a 7° beam width and operated with a pulse length of 1024  $\mu$ s. In Monterey Bay, data were collected from two platforms: the RV Martin with all three frequencies hull mounted and pinging continuously and the RHIB Musculus with 38 and 120 kHz transducers pole mounted, running on Ek80 CW mode, and deployed opportunistically when the vessel was available and in the vicinity of tagged whales. On both Monterey Bay vessels, the 38 kHz transducer had a beam width of 12° and used a 1024  $\mu$ s pulse length and other transducers had 7° beam width with a 512  $\mu$ s pulse length. Bottom depth in all South Africa humpback whale habitat was < 150 m, above the time-varied gain noise threshold for the 200 kHz transducer at -80 dB. All units reported in dB are  $S_v$  (mean volume backscatter strength) re 1 m<sup>2</sup>/m<sup>3</sup>, except when specifically referencing individual target strength (TS), which is reported in dB re 1 m<sup>2</sup>, and when  $S_a$  is reported in Fig. S2, which is in dB re 1 m<sup>2</sup>/m<sup>2</sup> (see MacLennan, Fernandes & Dalen 2002 for details). Because the 120 kHz transducer was not operable for the bulk of analysis days in South Africa and the 200 kHz had sufficient resolution for the depths of interest (no data deeper than 150 m), for consistency across that ecosystem the 120 kHz data from its five functional days was excluded. In contrast, blue whale habitat was deeper (bottom depth often > 400 m, with dives to krill patches up to 250 m deep), so the 120 kHz was used as the primary comparison to 38 kHz data (which also allowed consistency across Monterey Bay vessels). Relative krill sizes in the two ecosystems (see below) also justified the analytical frequencies.

All systems were calibrated using a 38.1 mm tungsten carbide sphere (Demer *et al.* 2015) as close as possible to the time of data collection. In both field sites this was immediately temporally adjacent to the

second field season for each of the large vessels (RV Martin and RV Khuzwayo) and within a week of all data collected on the Musculus. Echosounders were set to ping between 0.5 to 1.5 s (typical values were 1-1.2 s) based on bottom depths. If false bottoms appeared in the monitored echograms, ping intervals were increased.

Humpback whale super-groups observed in South Africa were tightly spaced (>50 whales in a square region <100-200 m on a side (Fig 2)). The limited maneuverability of the 39 m RV Khuzwayo precluded entry directly into these tight formations, so prey mapping around whales consisted of doing box patterns at distances of 100-500 m from the main group. On one occasion on 3 Nov 2016 the group moved within 100 m of the vessel and forward motion was halted. Due to weather conditions and equipment delays, only one tagged humpback whale foraging in a super-group overlapped with prey mapping around super-groups (Fig 2E), so prey and whale analysis are generally from different super-groups. Blue whale super-groups observed in Monterey Bay were more loosely aggregated and could be maneuvered among, so prey data during super-group events are in and among foraging whales, and six tagged whales fed for at least part of their tagged duration within super-groups (Table S2). Due to competing research priorities, the areas surveyed were at times haphazard, so we could not attempt analyses that depended on the horizontal spatial extent of prey layers but instead focused on prey density near super-groups in comparison to prey density near feeding whales that were not in super-groups.

### *Prey data processing*

Hydroacoustic data were imported into Echoview 9 and each field day was analyzed independently. Standard acoustic processing resulted in the removal of data below the sea floor, general background noise (De Robertis & Higginbottom 2007), additional regions of high noise (common when the ship was maneuvering or in rough seas) and signals from other sonar systems (Ryan *et al.* 2015) across all frequencies. The geometry of the high-frequency (HF, 120 or 200 kHz) and 38 kHz data were matched, and the SHAPES algorithm for school detection (Barange 1994; Coetzee 2000) was applied to a HF-38 dB differenced echogram thresholded at 8 dB (see rationale below).

Mean krill lengths in both ecosystems under study were substantially smaller than the mean lengths of *Euphausia superba* on which the majority of euphausiid hydroacoustic literature focuses (techniques summarized in Jarvis *et al.* 2010). While *E. superba* have seasonal mean lengths that range from 30 to 50 mm (Atkinson *et al.* 2009), measured *E. lucens*, the dominant euphausiid in South Africa, during a cruise concurrent to our field efforts were  $14 \pm 1.4$  mm, and adult *E. pacifica* and *Thysanoessa spinifera*, the dominant Euphausiids in Monterey Bay (Croll *et al.* 2009) and in blue whale diets (Croll *et al.* 2005; Nickels, Sala & Ohman 2018) range from  $10.2 \pm 3.0$  to  $16.0 \pm 2.0$  mm and  $15.3 \pm 0.2$  to  $23.7 \pm 0.4$  mm, respectively, with krill in blue whale fecal samples consistently larger than those found in net tows (Croll *et al.* 2005; Nickels, Sala & Ohman 2019). At a nominal sound speed of  $1500 \text{ m s}^{-1}$  the wavelengths of 38, 120 and 200 kHz signals are 39.5, 12.5 and 7.5 mm respectively, implying that for zooplankton lacking a resonator (like an air-filled swim-bladder), animals smaller than the wavelength of the signal will have strongly reduced signals (Stanton *et al.* 1994; Stanton, Chu & Wiebe 1998) and additionally implying that dB differencing and target strength (TS) models for larger krill like *E. superba* are not appropriate for the smaller krill in this study. Instead, TS of these krill were calculated using an SDWBA scattering model (as in Conti & Demer 2006), but parameterized with inputs (e.g., animal density and sound speed relative to seawater and krill morphology) measured on krill species which are found in the Monterey Bay study site, *T. spinifera* and *E. pacifica*, and also applied to the similarly-sized *E. lucens*. An average TS for each ecosystem was calculated by averaging (in the linear domain) 1000 simulated krill with lengths from normal distributions determined from representative krill sizes. For *E. lucens* we used our measured lengths, and for Monterey Bay data we used the fecal-sample-determined distribution of *T. spinifera* (the most common blue whale prey as per Nickels, Sala & Ohman 2018; Nickels, Sala & Ohman 2019) from Croll *et al.* (2005) of  $19.3 \pm 1.5$  mm. Using *E. lucens* length-wet weight curves (Pérez Seijas 1987) and averaging male and female values gave 0.026 g/krill, similar to the 0.025 g/krill derived from a cross-species relationship (Mauchline 1967). We applied the smaller value since our mean sizes were larger than the juvenile *E. lucens* data measured by Pérez Seijas. *T. spinifera* wet weight (0.040 g/krill) was also calculated from the Mauchline curve but restricted to Pacific Ocean *Thysanoessa sp.* and *E. pacifica* measurements. TS

calculated from these lengths and our SWDBA model were -93.2 (@120 kHz) and -93.6 dB re 1 m<sup>2</sup> (@200 kHz) for Monterey Bay *T. spinifera* and South Africa *E. lucens* respectively. At these size ranges, HF minus 38 kHz dB differences ranged from 16-18 dB in Monterey Bay and 23-24 dB in South Africa (mean size  $\pm$  2 *SD*). Mean biomass density (*B*) in kg/m<sup>3</sup> at any spatial scale could then be estimated via eq. 1 (as described in Simmonds & MacLennan 2008; Jarvis *et al.* 2010) from the measured mean volumetric backscatter at the corresponding spatial scale (*S<sub>v</sub>*), the estimated TS and the estimated individual krill mass (*M*) in g:

$$B = \frac{10^{S_v/10}}{10^{TS/10}} \times \frac{M}{1000} \quad (\text{eq. 1})$$

At high frequencies (120 and 200 kHz), euphausiid TS are highly susceptible to changes in orientation, with, for instance, orientation changes of five degrees potentially resulting in 200 kHz TS differences up to 20 dB (Demer & Martin 1995; Stanton & Chu 2000; CCAMLR 2005). Additionally, these relatively large dB differences (compared to the differences centered around 9 dB for *E. superba*, Jarvis *et al.* 2010) often spanned to levels below the detection threshold used for 38 kHz analysis. Consequently, for exclusion of likely non-euphausiid backscatter, a lower threshold of 11.4 dB was used for 200 kHz data and 9.5 dB for 120 kHz data so that krill would not be inappropriately excluded (Warren *et al.* 2001). These thresholds are the mean of the low value used for *E. superba* (Jarvis *et al.* 2010) and the HF-38 differences for the largest krill we measured (18.7 dB at 200 kHz, 14.3 dB at 120 kHz for 35 mm *T. spinifera*). These values should allow our results to be comparable to previous studies that used lower thresholds and also confirmed high krill abundances (using net tows) collocated with high acoustic backscatter in Monterey Bay (Schoenherr 1991; Croll *et al.* 2009; MBNMS 2009; Santora, Ralston & Sydeman 2011).

Siphonophores are known contributors to acoustic backscatter and their presence can bias results (Warren *et al.* 2001; McGarry 2014). To minimize this source of error, we linearly subtracted the backscatter at 38 kHz from the HF backscatter; since siphonophores have resonant air pockets they have similar backscatter at HF as at 38 kHz (Stanton, Chu & Wiebe 1998; Warren *et al.* 2001). All *S<sub>v</sub>* reported are this linearly subtracted value, which were  $0.2 \pm 0.3$  dB and  $0.1 \pm 0.1$  dB lower than the HF values in Monterey Bay and South Africa respectively.

### *Distribution of resources*

To confirm that gulp-sized cells, our base analytical unit, were distributed lognormally, histograms of biomass in gulp-sized cells were examined on a day-by-day basis and in total (Fig. S1). Although most statistical tests for normality are not appropriate for large sample sizes – e.g. total gulp-sized patches within an ecosystem – and are sensitive to outliers (Ghasemi & Zahediasl 2012), a Box Cox transformation on krill density in all gulp-sized cells resulted in a parameter of 0, suggesting the appropriateness of log transforming biomass. For each krill patch identified, a signed rank-sum test comparing the median of all of the gulps within a patch to the overall biomass derived from patch  $S_v$  revealed that in three quarters of the cases, gulp medians were significantly different than the linearly averaged  $S_v$  of the patch (Fig. S1), suggesting that resources the size of what whales actually feed on (the gulp-sized cell) are not represented by the patch arithmetic mean. Given the lognormal distributions of gulps within patches, the variation in patch sizes, and the variation in the number of acoustic samples per patch in our acoustic surveys, the commonly employed approach of linearly averaging all acoustic data within whole patches or large cells into single values would be likely to skew the data to a degree dependent on the size of the patches and the preponderance of any rare but large data that are unlikely to be encountered by a foraging predator (i.e. outliers).

As an additional line of evidence to determine if there would be a difference between analyzing ecosystem data using gulp-sized cells compared to mean patch densities, we looked at the distributions of gulps within krill patches and used a nonparametric rank-sum test to test if the patch  $S_v$  were likely to have been sampled from the observed distribution of gulp sizes. The frequency of times when the null hypothesis could be rejected on each day is shown in Fig S1 and demonstrated significance in 505 of 1422 tests ( $p$  from Fisher's combined probability test = 0). We also performed the same test for the  $S_v$  of dive-sized cells within krill patches and found that only 24 of 1325 krill patches rejected the null hypothesis (Fisher's  $p$ -value = 1). This suggested that the distributions of gulps within a krill patch were often significantly different than the linearly averaged mean value in the patch. To remove any outliers due to acoustic noise

(including missing data due to dropped pings) that were missed during the data preparation process, the lowest and highest 0.5% of each day's gulp sized cells were removed from analysis.

#### *Additional tests for acoustic artefacts*

The “whale scale” level of analysis – the primary analytical scale – includes comparisons of gulp-sized cells both horizontally (across pings) and vertically (within pings). When ensonifying dense swarms, care must be taken to ensure that neither artefacts due to extinction (e.g. Foote 1990), nor artefacts in the opposite direction due to multiple scattering (Stanton 1983) influence results. In some cases these two artefacts may offset (Stanton 1983), but in both cases they are more prevalent when ensonifying organisms with stronger TS. These effects are mostly relevant when enumerating fish (with TS ~ -50 to -20 dB, Foote 1980) but have been observed to lesser extents in larger krill species like *E. superba* (TS @ 40 mm ~ -77 dB, Conti & Demer 2006), and are not commonly reported with extremely small TS of the krill in our ecosystem (~-93 dB). However, to confirm that our results are not influenced by these effects, we examined both gulp density as a function of location in the water column as well as the strength of the bottom return echo in dense krill and outside of dense krill. If gulp depth is plotted against  $S_{v\_gulp}$ , no relationship is noted ( $r^2 = 0.036$ ), and if a Generalized Linear Mixed Effects model (GLME) is run treating each column of data as a random effect, a slightly increasing relationship is noted (slope estimate 0.08 dB/gulp height,  $p < 0.001$ ) implying that any extinction effect would be small. When examining the bottom echo, we calculated the strength of all bottom echoes for data from 05 Nov 2015, the day shown in Fig. 4, in which we recorded some of the strongest returns near the bottom that would be strong candidates to demonstrate acoustic artefacts (if they were present). Bottom return in each ping was calculated in two ways: as the sum of scattering ( $S_a$ ) from 0.5 to 5.5 m below the sounder detected bottom, and as the 95<sup>th</sup> percentile of 0.1 m  $S_v$  bins in the same depth window. Comparisons of bottom strength in strongly scattering regions to adjacent regions were either not significantly different or had small differences in opposing directions (Fig S2). We also compared  $S_a$  in that 5 m bin below the bottom line to  $S_a$  in the water column above the line (down to 1.5 m above the line) in Fig S3 and found nearly no relationship. The small size of these effects, combined

with the inconsistent direction, suggests that any effect would be small and less than the error of the estimates of the means in the whale scale analysis. When applying our approach to new ecosystems with more reflective target organisms, similar precautions should be taken.

Similarly, the stochasticity inherent in acoustic data suggests that precautions should be taken to ensure that gulp-sized cells are large enough to include sufficient pings to accurately represent biomass (Foote 1983; Simmonds & MacLennan 2008). Our gulp-sized cells in Monterey averaged  $9.4 \pm 12.5$  pings (mean  $\pm$  *SD*), while in South Africa humpback whale gulp-sized cells averaged  $8.4 \pm 6.8$  pings. To ensure cells with only a single ping were never used, in South Africa all pairs of pings were averaged into a single ping using the ping-reduction feature in Echoview. It was subsequently determined that this step made for more complicated post-processing as different ping indices were then employed for the analysis of raw and processed data. In Monterey data processing, then, an updated approach was used to simplify post-processing. All data was extracted in gulp-sized cells, but then any cell containing only a single ping was averaged into the subsequent cell (and that cell's ping number was increased by one).

Finally, it should be noted that there are many avenues for error propagation when converting acoustic backscatter to biomass: krill, which can swarm facing any direction (Calise 2009), have orientation-dependent TS (Conti & Demer 2006; Levine, Williams & Ressler 2018), efforts to ground truth estimates are inhibited by unknown krill escape from nets (Everson & Bone 1986; Brierley 1999) which may be size dependent (Hill *et al.* 1996), even with concurrent net-sampling the krill ensounded may be of different size classes than the krill sampled, krill may be oriented in different directions throughout a swarm (Hamner & Hamner 2000), and all models are subject to normal stochastic variation (Simmonds & MacLennan 2008). In any distribution, the multiplicative geometric mean and GSD will be more robust to some of these errors than linear summary statistics.

We report derived biomass units using the best available techniques as they are the most biologically relevant, but we also report the directly measured backscatter data in all cases so that any future improved models may be retroactively applied, including models that may directly link acoustic backscatter of krill with energy content, as proposed in Benoit-Bird and Au (2002). For comparability, all statistical

comparisons were based on log-transformed data ( $S_v$  data before biomass conversion) and were only performed within (not across) ecosystems.

### *Estimating overall intake*

The whale scale method described herein is recommended for describing the distribution of resources within large patches or within a larger region. Calculating the distribution of biomass within cells the size of a whale's dive gives a representation of the likelihood that prey of a given biomass is encountered by a foraging whale, and reporting summary variables of lognormal distributions allows distributions in different environments to be statistically compared. However, a whale foraging in this environment will consume on average more biomass per gulp than the geomean biomass due to the right-skew of the lognormal distribution (i.e., the mean of a lognormal distribution is higher than its geomean which is equivalent to the median). If a whale samples randomly from a given dive-sized cell, the expected amount of prey consumed would be given by the number of lunges ( $n$ ) multiplied by the arithmetic mean biomass of the cell ( $B_{dive}$ ).  $B_{dive}$  can be estimated from the geomean and GSD parameters of the lognormal distribution of biomass in gulp-sized cells ( $B_{gulp}$ ). If we define parameters  $\mu = \log(\text{geomean}(B_{gulp}))$  and  $\sigma = \log(\text{GSD}(B_{gulp}))$  to be the mean and standard deviation of  $\log(B_{gulp})$  in a dive-sized cell, then the estimated mean biomass density engulfed by a randomly lunging whale (denoted  $\widehat{B}_{dive}$  to signify that it is a calculated parameter derived from the distribution) can be calculated from these parameters using any of these equivalent formulas for the expectation of the lognormal distribution:

$$\widehat{B}_{dive} = e^{\mu + \sigma^2/2} = e^{\mu \cdot \log(b) + (\sigma \cdot \log(b))^2/2} = e^{\log(\text{geomean}) + (\log(\text{GSD}))^2/2} \quad (\text{eq. 2})$$

where  $b$  is the base of the logarithm used to calculate  $\mu$  and  $\sigma$  and “log” is the natural logarithm. If we wish to estimate the linearized mean of acoustic backscatter from  $\text{mean}(S_{v\_gulp})$  and  $SD(S_{v\_gulp})$ , i.e., the parameters of  ${}_N S_{v\_ws}$ , directly without first back transforming to linear units, it can be derived from eq. 2 that:

$$\widehat{S_{v\_dive}} = \text{mean}(S_{v\_gulp}) + \left( SD(S_{v\_gulp}) \right)^2 \cdot \frac{\log(10)}{20} \quad (\text{eq. 3})$$

Calculating  $\hat{B}$  directly using eq. 2 or indirectly using the results of eq. 3 would be equivalent to directly calculating the mean biomass if biomass data were perfectly lognormally distributed. In natural environments, calculating  $\hat{B}$  from distribution parameters may be more robust than calculating mean biomass directly since lognormal parameters are more robust to outliers and acoustic artefacts. Summarizing data at spatial scales relevant to predators is also more likely to reflect the mean prey encountered by predators (Haeckel 1893; Stephens & Krebs 1986) than, for instance, averaging patches of different sizes or looking at the mean of all patches combined. Thus, the biomass expected to be consumed from a randomly foraging predator could be calculated from eq. 2 using the geomean and GSD of all  $\widehat{B}_{dive}$  (or, equivalently, the mean and  $SD$  of  $\widehat{S}_{v\_dive}$ ) in a region. Because predators are likely to forage with some degree of discrimination about what part of a patch they forage in, we suggest that biomass calculated as described above would be a lower bound for an estimate of consumption, while employing the same procedure using parameters at the informed whale scale (using only the densest half of gulp-sized cells within dive-sized cells) could be a more accurate estimate.

## Figures & Tables

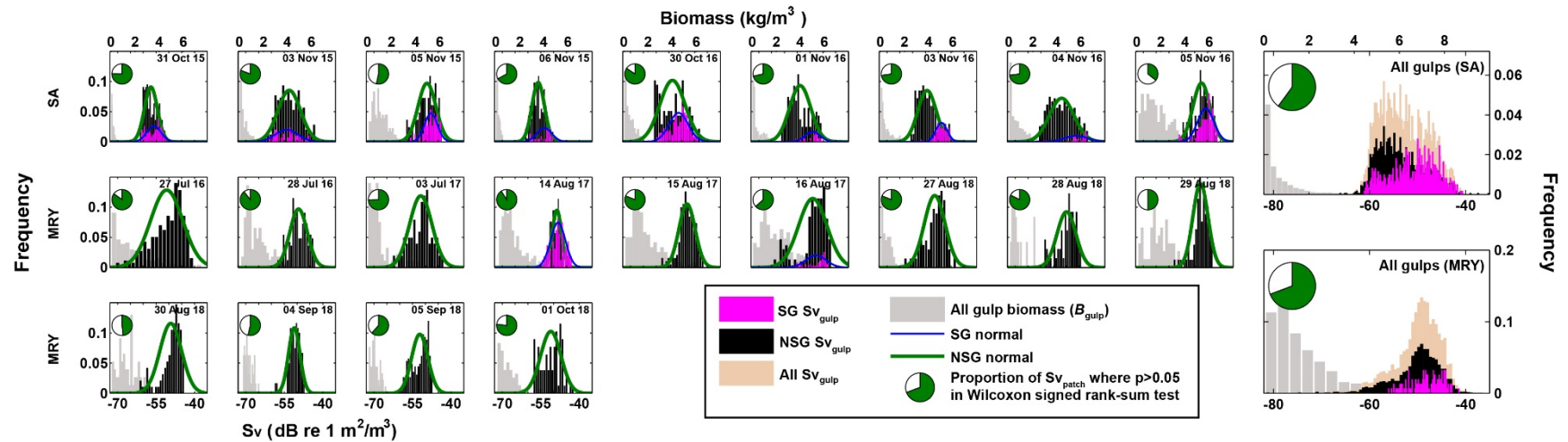


**Fig. S1-** Distribution of gulp sized cells of acoustic energy (tan, black and magenta) bars and biomass (grey bars) for each day. Acoustic energy (described in logarithmic units) is approximately normally distributed while biomass is skewed. Green pie charts show the proportion of identified krill patches that day for which the null hypothesis, that the distribution of Sv<sub>gulp</sub> within the patch is centered around Sv<sub>patch</sub>, could not be rejected at the  $p < 0.05$  significance level according to the Wilcoxon signed rank-sum test.

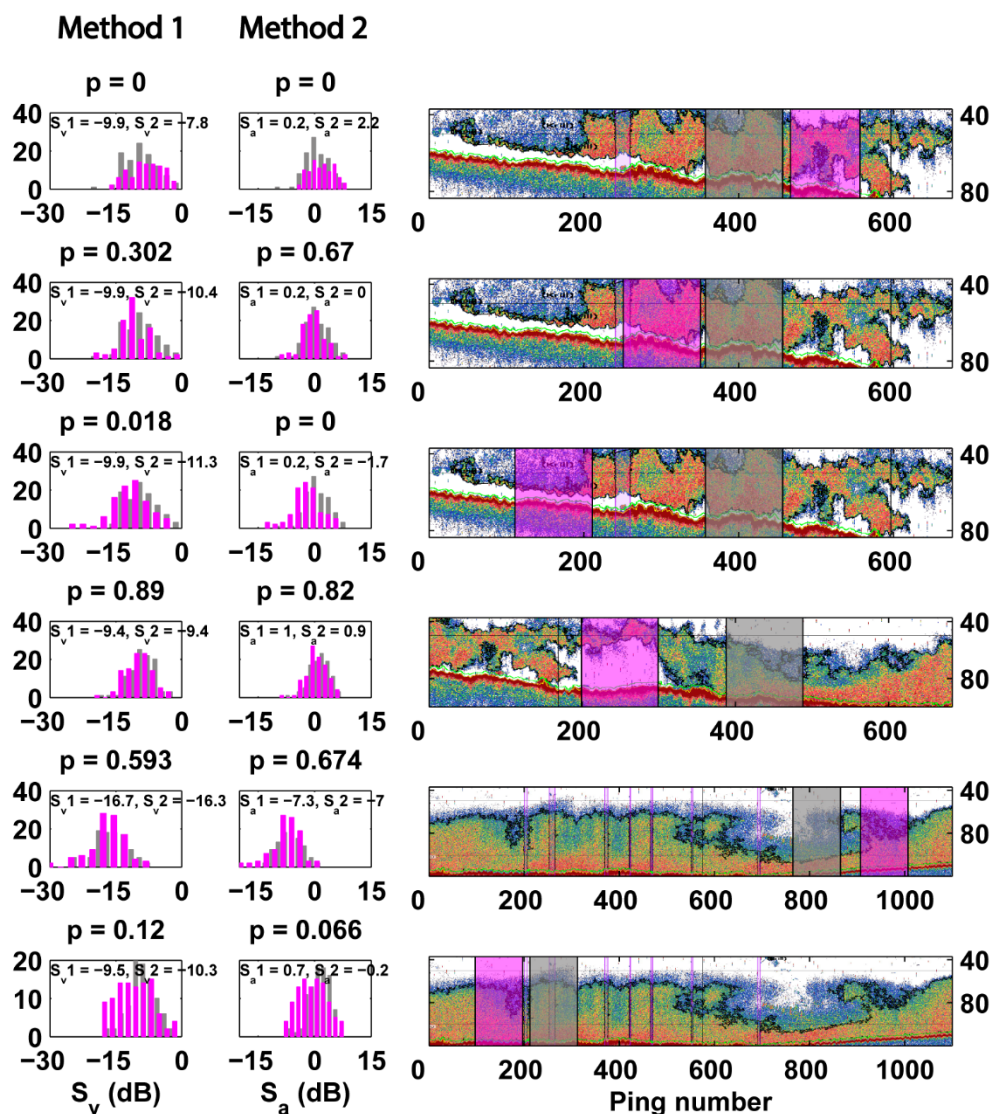


**Fig. S2-** Comparisons of bottom echo strength in adjacent regions of varying water column echos, for determining if there is an acoustic shadowing effect from dense scatterers. Gray regions have higher water column strength and pink regions have lower water column strength, histograms are plots of all pings in the highlighted regions. Method 1- the 95<sup>th</sup> percentile of 0.1 m  $S_v$  bins 0.5 to 5.5 m below the sounder-detected bottom for each ping. Method 2- the sum of scattering ( $S_a$ ) from 0.5 to 5.5 m below the sounder-detected bottom. Data was collected at 200 kHz data on 05 Nov 2015.

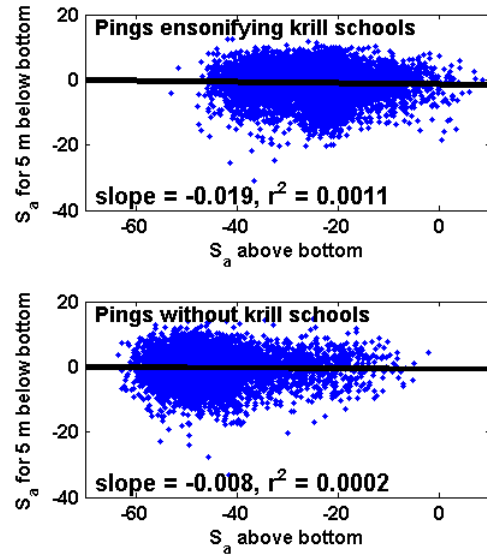


**Fig. S3-** Plots of  $S_a$  for each 200 kHz ping on 05 Nov 2015 from 0.5 to 5.5 m below the sounder-detected bottom as a function of  $S_a$  in the water column. The flat lines suggests no (or very minimal) acoustic shadowing effects.

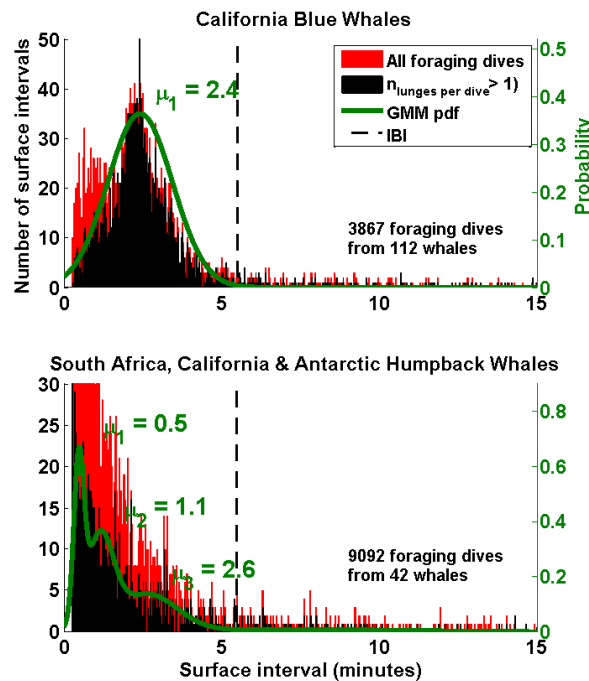


**Fig. S4-** Surface interval between foraging dives for blue whales and humpback whales tagged in multiple ecosystems. Black bars are surface intervals from foraging dives with at least 2 lunges until the next foraging dive. Red is the surface intervals for all foraging dives. For both species, the surface interval duration corresponding to the mean of the largest fitted Gaussian curve in the bulk of the data + 3  $SD$  was used to differentiate “foraging bouts.” That is, a “foraging bout” was defined as the combined duration of all dives where the surface interval between dives with foraging effort was less than 5.5 minutes (the dashed vertical bar in both plots). The duration of a foraging bout was defined from the start of the first dive to 5.5 minutes after the last foraging dive.

**Table S1-** Summary of data collected near super-groups (SG)

<i>Region</i>	<i>Date</i>	<i>Hrs prey mapping near SG</i>	<i>Hrs prey mapping near feeding whales not in SG</i>	<i>Estimated SG size (best estimate number of animals)</i>	<i>Time prey data collection around SG began</i>	<i>Number of tagged whales in SG (total hrs)</i>
<b>South Africa</b> ( <i>M. novaeangliae</i> )	31-Oct-2015	1.3	3.5	50	13:08	2 (4.5)
	3-Nov-2015	0.6	10.2	—	20:42	1 (3.7)
	5-Nov-2015	0.8	1.1	150	17:41	0 (—)
	6-Nov-2015	0.9	3.8	25	8:04	0 (—)
	30-Oct-2016	0.9	7.6	45	18:32	0 (—)
	1-Nov-2016	0.7	2.5	60	8:34	0 (—)
	3-Nov-2016	3.9	4.2	80	7:33	0 (—)
	4-Nov-2016	0.9	6.3	60	9:53	0 (—)
	5-Nov-2016	2.0	2.8	50	7:07	1 (0.9)
	6-Nov-2016	—	—	50	—	1 (5.7)
	7-Nov-2016	—	—	75	—	1 (1.7)
<b>Monterey</b> ( <i>B. musculus</i> )	14-Aug-2017	0.9	1.8	25	10:19	2 (5.0)
	16-Aug-2017	0.8	5.0	15	13:32	4 (5.5)
	Combined other days	—	32.3	—	—	—

**Table S2-** Feeding parameters from tag data for individual whales while they were foraging in super-groups compared to when they were not within a super-group. Each row is a unique tag ID of the format spYYMMDD-tag#, where sp = species ID (mn for humpback whales, bw for blue whales), year, month, day and tag number.

<b><i>M. novaeangliae</i> (South Africa)</b>								
<i>Tag ID</i>	<i>Feeding rate (lunges per hr within a feeding bout)</i>		<i>Inter lunge interval (ILI, s)</i>		<i>Inter lunge search area (<math>10^2 m^2</math>)</i>		<i>Lunges per dive</i>	
	SG	NSG	SG	NSG	SG	NSG	SG	NSG
mn151031-3	58.3	—	34 ± 8	—	3.1 ± 1.3	—	6.7 ± 2.1	—
mn151031-4	62.7	63.8	30 ± 9	35 ± 9	3.9 ± 2.6	4.7 ± 4.4	6.2 ± 1.4	2.9 ± 1.0
mn151103-7	77.3	45.1	33 ± 11	39 ± 20	3.3 ± 3.2	9.2 ± 14.5	3.7 ± 1.9	7.6 ± 3.5
mn161105-36	37.5	20.5	32 ± 9	33 ± 34	4.0 ± 3.0	—	3.8 ± 0.9	2.5 ± 0.7
mn161106-36b	55.9	21.3	32 ± 10	70 ± 30	4.0 ± 2.4	11 ± 9.3	3.5 ± 1.3	2.9 ± 0.8
mn161107-36b	38.5	35.3	31 ± 10	21 ± 3	2.3 ± 0.8	—	2.9 ± 1.0	2.2 ± 0.4
<b><i>B. musculus</i> (Monterey Bay)</b>								
<i>Tag ID</i>	SG	NSG	SG	NSG	SG	NSG	SG	NSG
bw170814-40	23.8	27.0	94 ± 13	93 ± 19	27 ± 14	39 ± 31	4.6 ± 1.1	3.5 ± 1.3
bw170814-50	22.6	19.4	96 ± 19	102 ± 17	51 ± 39	54 ± 27	4.0 ± 0.9	3.1 ± 0.9
bw170816-23	29.2	—	81 ± 8	—	33 ± 12	—	4.2 ± 0.4	—
bw170816-42	21.1	14.2	103 ± 23	104 ± 6	40 ± 46	38 ± 6.3	3.1 ± 1.0	2.8 ± 1.3
bw170816-44	26.1	24.8	89 ± 17	101 ± 21	49 ± 46	51 ± 65	3.9 ± 0.6	3.4 ± 1.6
bw170816-51	22.6	18.4	107 ± 5	111 ± 13	17 ± 1.6	29 ± 16	4.0 ± 0.6	3.9 ± 1.2

**Table S3-** Prey in super group (SG) regions and in regions where whales are present but not aggregated (NSG). SA = South Africa, MRY = Monterey.

<b>Panel A: Humpback whales</b>												
<i>Date of SG</i>	<i>Patch biomass</i> ( $LN B_{patch}$ ) in $kg m^{-3}$ ( $NS_V patch$ in dB)		<i>Whale scale biomass</i> ( $LN B_{WS}$ ) in $kg m^{-3}$ ( $NS_V WS$ in dB)		<i>Informed whale scale</i> (informed $LN B_{WS}$ ) in $kg m^{-3}$ (informed $NS_V WS$ in dB)		<i>Patch thickness (m)</i>		<i>Whale scale SD</i> (dB)		<i>Informed whale scale SD</i> (dB)	
	SG	NSG	SG	NSG	SG	NSG	SG	NSG	SG	NSG	SG	NSG
31-Oct-2015	0.12 : 1.8 * (-56.8 ± 2.4)	0.09 : 1.7 (-58.1 ± 2.2)	0.17 : 1.7 *** (-55.2 ± 2.3)	0.14 : 1.8 (-56.3 ± 2.4)	0.27 : 1.3 ** (-53.2 ± 1.2)	0.24 : 1.4 (-53.8 ± 1.5)	23 ± 12 ***	10 ± 8	2.3	2.4	1.2 ***	1.5
3-Nov-2015	<i>0.19 : 2.5</i> (-54.7 ± 4.1)	<i>0.29 : 2.8</i> (-53.0 ± 4.4)	<i>0.27 : 2.2</i> (-53.3 ± 3.3)	<i>0.32 : 2.1</i> (-52.6 ± 3.3)	0.66 : 1.5 * (-49.4 ± 1.6)	0.51 : 1.6 (-50.6 ± 2.0)	21 ± 15 ***	3 ± 3	3.3	3.3	1.6 ***	2.0
5-Nov-2015	<i>0.33 : 4.3</i> (-52.4 ± 6.3)	<i>0.34 : 2.2</i> (-52.3 ± 3.5)	0.84 : 1.9 * (-48.3 ± 2.8)	0.61 : 2.2 (-49.7 ± 3.4)	1.39 : 1.3 * (-46.2 ± 1.3)	1.15 : 1.5 (-47.0 ± 1.6)	37 ± 10 ***	23 ± 13	2.8	3.4	1.3 ***	1.6
6-Nov-2015	0.22 : 2.2 (-54.1 ± 3.5)	0.13 : 1.7 (-56.5 ± 2.4)	0.27 : 2.0 *** (-53.3 ± 3.0)	0.15 : 1.9 (-55.7 ± 2.7)	0.47 : 1.4 *** (-50.9 ± 1.3)	0.27 : 1.4 (-53.3 ± 1.5)	30 ± 19 ***	8 ± 7	3.0	2.7	1.3 ***	1.5
30-Oct-2016	0.45 : 2.1 ** (-51.1 ± 3.3)	0.21 : 3.3 (-54.4 ± 5.2)	0.46 : 2.4 (-50.1 ± 3.8)	0.28 : 2.2 (-53.1 ± 3.5)	1.07 : 1.5 (-47.3 ± 1.8)	—	8 ± 5 ***	3 ± 2	3.8	3.5	1.8	—
1-Nov-2016	0.84 : 1.6 *** (-48.4 ± 2.1)	0.17 : 2.2 (-55.2 ± 3.4)	0.59 : 2.1 * (-49.9 ± 3.3)	0.35 : 2.8 (-52.2 ± 4.4)	<i>1.34 : 1.4</i> (-46.3 ± 1.4)	<i>1.46 : 1.6</i> (-46.0 ± 2.0)	15 ± 7 ***	6 ± 5	3.3	4.4	1.4 ***	2.0
3-Nov-2016	0.75 : 1.8 *** (-48.8 ± 2.7)	0.15 : 2.0 (-55.8 ± 3.0)	0.70 : 1.9 *** (-49.2 ± 2.8)	0.29 : 2.1 (-53.0 ± 3.3)	1.14 : 1.3 *** (-47.0 ± 1.1)	0.63 : 1.4 (-49.6 ± 1.5)	34 ± 7 ***	8 ± 7	2.8	3.3	1.1 ***	1.5
4-Nov-2016	1.56 : 3.3 ** (-45.7 ± 5.2)	0.25 : 2.7 (-53.7 ± 4.3)	1.23 : 2.3 *** (-46.7 ± 3.6)	0.51 : 2.3 (-50.5 ± 3.6)	2.31 : 1.4 *** (-44.0 ± 1.4)	1.28 : 1.5 (-46.5 ± 1.6)	23 ± 8 ***	7 ± 8	3.6	3.6	1.4 ***	1.6
5-Nov-2016	1.22 : 2.3 (-46.7 ± 3.6)	1.05 : 2.9 (-47.4 ± 4.7)	1.11 : 2.3 * (-47.1 ± 3.5)	0.82 : 2.4 (-48.4 ± 3.8)	2.15 : 1.4 ** (-44.3 ± 1.4)	1.75 : 1.4 (-45.2 ± 1.6)	19 ± 8 ***	14 ± 7	3.5	3.8	1.4 ***	1.6
All SA	0.35 : 3.4 *** (-52.1 ± 5.3)	0.18 : 2.6 (-55.1 ± 4.2)	0.49 : 2.0 *** (-50.7 ± 3.0)	0.31 : 2.1 (-52.7 ± 3.3)	0.91 : 1.3 *** (-48.0 ± 1.3)	0.66 : 1.4 (-49.4 ± 1.6)	22 ± 14 ***	8 ± 9	3.0 **	3.3	1.3 ***	1.6
<b>Panel B: Blue whales</b>												
<i>Date of SG</i>	SG	NSG	SG	NSG	SG	NSG	SG	NSG	SG	NSG	SG	NSG
14-Aug-2017	0.84 : 2.0 (-50.0 ± 3.0)	1.09 : 1.8 (-48.9 ± 2.5)	1.38 : 1.6 * (-47.8 ± 2.0)	1.07 : 1.7 (-48.9 ± 2.2)	1.95 : 1.3 *** (-46.3 ± 1.0)	1.41 : 1.3 (-47.7 ± 1.3)	24 ± 24 ***	14 ± 14	2.0	2.2	1.0 ***	1.3
16-Aug-2017	0.95 : 2.8 (-49.4 ± 4.5)	0.70 : 4.5 (-50.8 ± 6.5)	1.74 : 1.7 (-46.8 ± 2.4)	1.54 : 1.8 (-47.3 ± 2.5)	2.74 : 1.3 *** (-44.8 ± 1.0)	2.35 : 1.3 (-45.5 ± 1.1)	50 ± 24 ***	20 ± 15	2.4	2.5	1.0 ***	1.1
All MRY	0.87 : 2.1 * (-49.8 ± 3.3)	0.67 : 3.7 (-50.9 ± 5.7)	1.49 : 1.6 *** (-47.5 ± 2.2)	1.19 : 1.8 (-48.5 ± 2.6)	2.22 : 1.3 *** (-45.8 ± 1.0)	1.89 : 1.3 (-46.5 ± 1.2)	33 ± 27 ***	15 ± 15	2.2 **	2.6	1.0 ***	1.2

Comparisons (\* =  $p < 0.05$ , \*\* =  $p < 0.01$ , \*\*\* =  $p < 0.001$ ). *Italics* indicates an effect in the opposite direction of the prevalence of data

— = data collected on this day did not meet the threshold of at least 30 gulps per dive



**Video S1-** On animal video from humpback whales foraging within super-groups. High quality version available with deposited data at: <https://purl.stanford.edu/rq794kc6747>

## References

- Atkinson, A., Siegel, V., Pakhomov, E., Jessopp, M. & Loeb, V. (2009) A re-appraisal of the total biomass and annual production of Antarctic krill. *Deep Sea Research Part I: Oceanographic Research Papers*, **56**, 727-740.
- Barange, M. (1994) Acoustic identification, classification and structure of biological patchiness on the edge of the Agulhas Bank and its relation to frontal features. *South African Journal of marine science*, **14**, 333-347.
- Benoit-Bird, K.J. & Au, W.W.L. (2002) Energy: Converting from acoustic to biological resource units. *The Journal of the Acoustical Society of America*, **111**, 2070-2075.
- Brierley, A.S. (1999) A comparison of Antarctic euphausiids sampled by net and from geothermally heated waters: insights into sampling bias. *Polar Biology*, **22**, 109-114.
- Cade, D.E., Barr, K.R., Calambokidis, J., Friedlaender, A.S. & Goldbogen, J.A. (2018) Determining forward speed from accelerometer jiggle in aquatic environments. *Journal of Experimental Biology*, **221**, jeb170449.
- Cade, D.E. & Benoit-Bird, K.J. (2014) An automatic and quantitative approach to the detection and tracking of acoustic scattering layers. *Limnology and Oceanography: Methods*, **12**, 742-756.
- Cade, D.E., Friedlaender, A.S., Calambokidis, J. & Goldbogen, J.A. (2016) Kinematic Diversity in Rorqual Whale Feeding Mechanisms. *Current Biology*, **26**, 2617-2624.
- Calise, L. (2009) Multifrequency acoustic target strength of northern krill.
- CCAMLR (2005) Report of the twenty fourth meeting of the Scientific Committee. SC-CAMLR-XXIV. *Commission for the Conservation of Antarctic Marine Living Resources*. <https://www.ccamlr.org/en/system/files/e-sc-xxix-a5.pdf>. Hobart, Australia.
- Coetzee, J. (2000) Use of a shoal analysis and patch estimation system (SHAPES) to characterise sardine schools. *Aquatic Living Resources*, **13**, 1-10.
- Conti, S.G. & Demer, D.A. (2006) Improved parameterization of the SDWBA for estimating krill target strength. *ICES Journal of Marine Science: Journal du Conseil*, **63**, 928-935.
- Croll, D.A., Marinovic, B., Benson, S., Chavez, F.P., Black, N., Ternullo, R. & Tershy, B.R. (2005) From wind to whales: trophic links in a coastal upwelling system. *Marine Ecology Progress Series*, **289**, 117-130.
- Croll, D.A., Newton, K.M., Marinovic, B.B. & Ralston, S. (2009) Critical Prey Species in the Monterey Bay National Marine Sanctuary. pp. 38. UC Santa Cruz.
- De Robertis, A. & Higginbottom, I. (2007) A post-processing technique to estimate the signal-to-noise ratio and remove echosounder background noise. *ICES Journal of Marine Science*, **64**, 1282-1291.
- Demer, D., Berger, L., Bernasconi, M., Bethke, E., Boswell, K., Chu, D. & Domokos, R. (2015) Calibration of acoustic instruments. *ICES Cooperative Research Report*, **326**, 133.
- Demer, D.A. & Martin, L.V. (1995) Zooplankton target strength: Volumetric or areal dependence? *The Journal of the Acoustical Society of America*, **98**, 1111-1118.
- Everson, I. & Bone, D. (1986) Effectiveness of the RMT8 system for sampling krill (*Euphausia superba*) swarms. *Polar Biology*, **6**, 83-90.
- Findlay, K.P., Seakamela, S.M., Meyer, M.A., Kirkman, S.P., Barendse, J., Cade, D.E., Hurwitz, D., Kennedy, A., Kotze, P.G.H., McCue, S.A., Thornton, M., Vargas-Fonseca, O.A. & Wilke, C.G. (2017) Humpback whale “super-groups” – A novel low-latitude feeding behaviour of Southern Hemisphere humpback whales (*Megaptera novaeangliae*) in the Benguela Upwelling System. *PLoS ONE*, **12**, e0172002.
- Foote, K.G. (1980) Averaging of fish target strength functions. *The Journal of the Acoustical Society of America*, **67**, 504-515.
- Foote, K.G. (1983) Linearity of fisheries acoustics, with addition theorems. *The Journal of the Acoustical Society of America*, **73**, 1932-1940.

- Foote, K.G. (1990) Correcting acoustic measurements of scatterer density for extinction. *The Journal of the Acoustical Society of America*, **88**, 1543-1546.
- Ghasemi, A. & Zahediasl, S. (2012) Normality tests for statistical analysis: a guide for non-statisticians. *International journal of endocrinology and metabolism*, **10**, 486.
- Goldbogen, J.A., Cade, D.E., Wisniewska, D.M., Potvin, J., Segre, P.S., Savoca, M.S., Hazen, E.L., Czapanskiy, M.F., Kahane-Rapport, S.R., DeRuiter, S.L., Gero, S., Tønnesen, P., Gough, W.T., Hanson, M.B., Holt, M., Jensen, F.H., Simon, M., Stimpert, A.K., Arranz, P., Johnston, D.W., Nowacek, D.P., Parks, S.E., Visser, F., Friedlaender, A.S., Tyack, P.L., Madsen, P.T. & Pyenson, N.D. (2019) Why whales are big but not bigger: Physiological drivers and ecological limits in the age of ocean giants. *Science*, **366**, 1367-1372.
- Goldbogen, J.A., Calambokidis, J., Shadwick, R.E., Oleson, E.M., McDonald, M.A. & Hildebrand, J.A. (2006) Kinematics of foraging dives and lunge-feeding in fin whales. *Journal of Experimental Biology*, **209**, 1231-1244.
- Haeckel, E. (1893) Planktonic studies: a comparative investigation of the importance and constitution of the pelagic fauna and flora. *Report of the US Commissioner of Fish and Fisheries for 1889 to 1893*, 565-641.
- Hamner, W.M. & Hamner, P.P. (2000) Behavior of Antarctic krill (*Euphausia superba*): schooling, foraging, and antipredatory behavior. *Canadian Journal of Fisheries and Aquatic Sciences*, **57**, 192-202.
- Hazen, E.L., Friedlaender, A.S. & Goldbogen, J.A. (2015) Blue whale (*Balaenoptera musculus*) optimize foraging efficiency by balancing oxygen use and energy gain as a function of prey density. *Science Advances*, **1**, e1500469.
- Hill, H., Trathan, P., Croxall, J. & Watkins, J. (1996) A comparison of Antarctic krill *Euphausia superba* caught by nets and taken by macaroni penguins *Eudyptes chrysolophus*: evidence for selection? *Marine Ecology Progress Series*, **140**, 1-11.
- Jarvis, T., Kelly, N., Kawaguchi, S., van Wijk, E. & Nicol, S. (2010) Acoustic characterisation of the broad-scale distribution and abundance of Antarctic krill (*Euphausia superba*) off East Antarctica (30-80 E) in January-March 2006. *Deep Sea Research Part II: Topical Studies in Oceanography*, **57**, 916-933.
- Johnson, M.P. & Tyack, P.L. (2003) A digital acoustic recording tag for measuring the response of wild marine mammals to sound. *IEEE Journal of Oceanic Engineering*, **28**, 3-12.
- Levine, M., Williams, K. & Ressler, P.H. (2018) Measuring the in situ tilt orientation of fish and zooplankton using stereo photogrammetric methods. *Limnology and Oceanography: Methods*, **16**, 390-399.
- MacLennan, D.N., Fernandes, P.G. & Dalen, J. (2002) A consistent approach to definitions and symbols in fisheries acoustics. *ICES Journal of Marine Science*, **59**, 365-369.
- Mauchline, J. (1967) Volume and weight characteristics of species of Euphausiacea. *Crustaceana*, 241-248.
- MBNMS (2009) Monterey Bay National Marine Sanctuary Condition Report 2009.
- McGarry, L. (2014) An Examination Of Blue Whale Foraging And Its Krill Prey Field In The Monterey Bay Submarine Canyon.
- Nickels, C.F., Sala, L.M. & Ohman, M.D. (2018) The morphology of euphausiid mandibles used to assess selective predation by blue whales in the southern sector of the California Current System. *Journal of Crustacean Biology*, **38**, 563-573.
- Nickels, C.F., Sala, L.M. & Ohman, M.D. (2019) The euphausiid prey field for blue whales around a steep bathymetric feature in the southern California current system. *Limnology and Oceanography*, **64**, 390-405.
- Pérez Seijas, G.M. (1987) Relaciones de talla, peso y volumen en *Euphausia vallentini*, *E. Lucens* y *Thysanoessa gregaria* (Euphausiacea, Eucarida).[*Euphausia vallentini*, *E. Lucens* and *Thysanoessa gregaria* (Euphausiacea, Eucarida) length, volume and weight relationships]. *Physica A*, **45**, 61-68.

- Ryan, T.E., Downie, R.A., Kloser, R.J. & Keith, G. (2015) Reducing bias due to noise and attenuation in open-ocean echo integration data. *ICES Journal of Marine Science*, **72**, 2482-2493.
- Santora, J.A., Ralston, S. & Sydeman, W.J. (2011) Spatial organization of krill and seabirds in the central California Current. *ICES Journal of Marine Science*, **68**, 1391-1402.
- Schoenherr, J.R. (1991) Blue whales feeding on high concentrations of euphausiids around Monterey Submarine Canyon. *Canadian Journal of Zoology*, **69**, 583-594.
- Simmonds, J. & MacLennan, D.N. (2008) *Fisheries acoustics: theory and practice*. John Wiley & Sons.
- Simon, M., Johnson, M. & Madsen, P.T. (2012) Keeping momentum with a mouthful of water: behavior and kinematics of humpback whale lunge feeding. *The Journal of Experimental Biology*, **215**, 3786-3798.
- Southall, B.L., DeRuiter, S.L., Friedlaender, A., Stimpert, A.K., Goldbogen, J.A., Hazen, E., Casey, C., Fregosi, S., Cade, D.E. & Allen, A.N. (2019) Behavioral responses of individual blue whales (*Balaenoptera musculus*) to mid-frequency military sonar. *Journal of Experimental Biology*, **222**, jeb190637.
- Stanton, T.K. (1983) Multiple scattering with applications to fish-echo processing. *The Journal of the Acoustical Society of America*, **73**, 1164-1169.
- Stanton, T.K. & Chu, D. (2000) Review and recommendations for the modelling of acoustic scattering by fluid-like elongated zooplankton: euphausiids and copepods. *ICES Journal of Marine Science*, **57**, 793-807.
- Stanton, T.K., Chu, D. & Wiebe, P.H. (1998) Sound scattering by several zooplankton groups. II. Scattering models. *The Journal of the Acoustical Society of America*, **103**, 236.
- Stanton, T.K., Wiebe, P.H., Chu, D., Benfield, M.C., Scanlon, L., Martin, L. & Eastwood, R.L. (1994) On acoustic estimates of zooplankton biomass. *ICES Journal of Marine Science: Journal du Conseil*, **51**, 505-512.
- Stephens, D.W. & Krebs, J.R. (1986) *Foraging theory*. Princeton University Press.
- Warren, J.D., Stanton, T.K., Benfield, M.C., Wiebe, P.H., Chu, D. & Sutor, M. (2001) In situ measurements of acoustic target strengths of gas-bearing siphonophores. *ICES Journal of Marine Science*, **58**, 740-749.
- Wilson, R.P., Liebsch, N., Davies, I.M., Quintana, F., Weimerskirch, H., Storch, S., Lucke, K., Siebert, U., Zankl, S. & Müller, G. (2007) All at sea with animal tracks; methodological and analytical solutions for the resolution of movement. *Deep Sea Research Part II: Topical Studies in Oceanography*, **54**, 193-210.

## Humpback and blue whale “super-groups” near dense, consistently distributed krill patches

*Cade, David; Seakamela, S. Mduduzi; Findlay, Ken; Fukunaga, Julie; Kahane-Rapport, Shirel; Warren, Joseph; Calambokidis, John; Fahlbusch, James; Friedlaender, Ari; Hazen, Elliott; Kotze, Deon; McCue, Steven; Mejer, Michael; Oestreich, William; Oudejans, Machiel; Wilke, Christopher; Goldbogen, Jeremy*

On Dec. 16, 1892, William S Bruce, a scientist aboard a whaling vessel near South Georgia Island on the edge of the Southern Ocean, observed thousands of fin and blue whales gathered close together: “Whale's backs and blasts were seen at close intervals quite near the ship, and from horizon to horizon.” Other contemporary accounts note similarly large aggregations, but by the latter half of the 20th century after intense commercial harvest that reduced populations to < 1% of historic abundances, groups of more than a handful of whales were rarely observed. Bruce himself notes that in 1912, more than 11,000 whales were killed in a single season by South Georgia whalers. Recently, however, large groups of densely aggregated blue whales have been reported off the California coast, and extraordinarily large groups of humpback whales (numbering upwards of 100-200 animals in a region 200 m on a side) have been observed in small patches of the ocean off South Africa’s west coast.

What draws these animals together? In both California and South Africa, abundant concentrations of krill are key prey for these large, lunge-feeding predators. In this work, we describe how krill patches near these super-groups are thicker, denser and more consistently distributed than other krill patches in the environment in which whales were observed foraging. We used video bio-logging tags to record the behavior of whales in these groups, and found that they fed more rapidly than whales not in super-groups, suggesting that prey was both high-quality and more

accessible such that whales did not have to traverse as far between high-quality mouthfuls.



Large, densely aggregated group of humpback whales, surfacing near Cape Town, SA © Dave Hurwitz

These large predators must navigate spatially and temporally patchy environments to find high-quality food during the limited foraging season. Our findings suggest that whales could potentially use cues from conspecifics to locate the best foraging environments, gathering in large numbers where prey is the most available. As populations continue to recover, we may see a positive feedback loop whereby more whales increase the ability of the whole population to find and detect prey.